Family Composition, Life Expectancy, and the Equilibrium Real Interest Rate*

Etienne Gagnon Benjamin K. Johannsen David López-Salido

May 15, 2016

Abstract

We calibrate an overlapping-generation model with a rich demographic structure to observed and projected changes in U.S. family composition and life expectancy from 1900 to 2100. The model accounts for a nearly $\frac{3}{4}$-percentage-point decline in the natural rate of interest since the 1980s—almost all of the permanent decline that has occurred since then according to some recent empirical estimates. We show that modeling the family structure is important for capturing the timing of that decline: Calibrations with dependent children point to the natural rate falling especially rapidly in recent and coming years, which suggests a risk that the permanent effects of demographic factors could be misinterpreted as persistent but ultimately transitory downward pressure on the natural rate of interest stemming from the Great Recession. The model also sheds light on the way demographic transitions will affect investment, real wages, and labor force participation.

JEL Codes: E17, E21, J11.

Keywords: Natural rate of interest, demographics.

*Federal Reserve Board. The views in this paper are solely the responsibility of the authors and should not be interpreted as reflecting the views of the Board of Governors of the Federal Reserve System or any other person associated with the Federal Reserve System. We are grateful to Carter Bryson and Kathryn Holston for excellent research assistance, and to seminar participants at the Bank of Canada. Comments and suggestions can be directed to etienne.gagnon@frb.gov, benjamin.k.johannsen@frb.gov, or david.lopez-salido@frb.gov.

1 Introduction

To support the economic recovery from the Great Recession, the Federal Reserve held the federal funds rate near zero and maintained large holdings of longer-term securities from late 2008 through 2015. Over that period, longer-term interest rates declined with little, if any, accompanying changes in measures of longer-term inflation expectations. That is, even as the unemployment rate fell from 10 percent to 5 percent, expected future real interest rates also fell, as figure 1 shows. Different causes of the decline in longer-term real rates have drastically different policy implications, making the cause of declining real rates an important concern for policymakers. Some observers, such as Summers (2014) and Gordon (2015), have argued that low longer-term real rates reflect secular stagnation or lower trend productivity growth. Others, like Rogoff (2015), point to persistent debt deleveraging and borrowing headwinds in the wake of the global financial crisis. Yet another possible contributing factor, suggested by the work of Blanchard and Fischer (1989), is that demographic changes have caused real rates to decline. The United States, like many other industrialized economies, has been experiencing dramatic demographic changes that will continue to unfold for several decades. This paper explores the extent to which these demographic changes can explain the timing and magnitude of movements in real interest rates during the post-war period and beyond.

To focus on the effects of demographic changes, we abstract from cyclical fluctuations. Movements in real interest rates that are not attributable to cyclical fluctuations are difficult to measure in the data. As a benchmark, we compare our model's implied equilibrium real interest rate to the measure of the real rate in the longer-run in Johannsen and Mertens (2016, shown in figure 2), which has the interpretation that it is the interest rate that would prevail absent transitory fluctuations. We find that an overlapping generation (OG) model calibrated to fit demographic data from 1900 to 2100 captures much of the permanent increase in real interest rates from 1960 to 1980 and almost all of the decline since.

Our model is based on the workhorse OG model that has notably been applied to the study of social security and generational accounting (see, for example, Reichlin and Smetters (2015)). Because we are interested in longer-term trends, we do not attempt to capture cyclical variation and assume that factor markets are frictionless and perfectly competitive. In our model, a household

lives for a finite number of periods, with the probability of death increasing with household age. Importantly, we assume no (intentional) bequest motive for our households. Without a sufficiently strong bequest motive, the finite lifespan of each household allows demographic transitions to influence real interest rates. By contrast, in a benchmark real business cycle (RBC) model in which households have infinite planning horizons, demographic transitions can have no such effect on real interest rates. We calibrate the probability of death using U.S. social security data. We augment our model with dependent children in a similar way to Chadwick *et al.* (2015a, 2015b); Browning and Ejrnæs (2009) show that adding children to the OG model helps to capture, in part or in all, the shape of consumption profiles of U.S. households with and without children. We calibrate the number of dependent children in our model based on U.S. fertility rates and find that including them has important implications for the size and timing of the decline in real interest rates over recent and coming decades.

A stark prediction of the model is that projected demographic changes over the next couple of decades will continue to put downward pressure on interest rates. Our model implies that the equilibrium real rate will fall permanently below 1 percent within the next decade. An important byproduct of this analysis is that the model predicts that net savings (net investment) rates, as well as the marginal product of capital, will also fall during that period. We find that these falls are driven by the ongoing decline in the labor supply due to population aging. Our projected fall in investment is consistent with older households persisting on capital savings, and dissaving during retirement. As investment falls, the capital-labor ratio slowly increases over the next two decades, and real wages (measured in efficiency units) accordingly rise. Over this same period, the labor-force participation rate declines about 3 percentage points for reasons related to demographic change.

We show that adding dependent children to our OG model implies that the most dramatic declines in the real interest rate and in investment have been occurring since the onset of the Great Recession. This finding is important because it suggests that real rates began to fall rapidly around the time of the global financial crisis in part because of underlying demographic transition, and not entirely because of cyclical weakness. Our results complement those reported in Ikeda and Saito (2014) and Carvalho *et al.* (2016). These studies focus on the distinction between working-age adults and retired adults, and show that a larger proportion of retired adults causes lower real

interest rates. We offer a richer demographic framework that includes dependent children, which we use to match both the size as well as the timing of changes in real interest rates over the past 60 years. Our model also delivers different conclusions regarding the relative importance of greater life expectancy and slower population growth for changes in real rates, relative to Carvalho *et al.* (2016).

2 Model economy

The economy is comprised of adults, dependent children, and representative firms. The children are introduced as in the recent work of Chadwick *et al.* (2015a, 2015b), which is based on Barro and Becker (1989). Adults are representative of their birth cohort in terms of life-cycle characteristics. Each period, these adults inelastically supply their labor endowments and decide how much they and their dependent children consume and how much to save for retirement. Representative firms operate a constant return to scale production technology that uses capital and labor inputs. Given our focus on low-frequency dynamics, we abstract from business cycle shocks and aggregate uncertainty; we instead assume that households and firms have perfect foresight with respect to aggregate variables and that they face no idiosyncratic risk besides the household's uninsurable risk of death. At the beginning of each period, children are born according to fertility rates that depend on the age and birth cohort of the adults. After children are born, some households members die, with probabilities conditional on age and birth cohort. After death, the remaining capital held by the household is uniformly redistributed to surviving adults. Finally, surviving adults make their consumption/saving decisions and firms produce.

2.1 Households

Consider a representative adult aged a in period t who has survived. Her problem is to maximize

$$\sum_{s=0}^{A-a} \beta^s \Gamma_{a,t,t+s} \left(\frac{\left(C_{a+s,t+s} - Z_{t+s}\bar{C}\right)^{1-\nu}}{1-\nu} + \epsilon \left(n_{a+s,t+s}\right)^{\eta} \frac{\left(C^c_{a+s,t+s} - Z_{t+s}\bar{C}^c\right)^{1-\nu}}{1-\nu} \right), \tag{1}$$

where $n_{a,t}$ is the number of dependent children, $C_{a,t}$ is the adult's consumption, and $C^c_{a,t}$ is the average consumption of each of its dependent children. As in Chadwick *et al.* (2015a, 2015b), we assume that parents derive utility from the their children's consumption. We also assume that parents and dependent children require subsistence levels of consumption, labeled $Z_t\bar{C}$ and $Z_t\bar{C}^c$,

respectively, which grow at the same pace as labor-augmenting technology, Z_t.[1] For tractability, we allow the number of dependent children to be fractional. The parameter $\epsilon \in [0,1]$ controls the weight placed by adults on their children's consumption whereas $\eta \in [0,1]$ captures the effects of family size on households utility. Adults derive utility only in periods in which they are alive, and have no bequest motive. The probability that an adult aged a in period t survives through the end of the next s periods is given by the cohort-specific function $\Gamma_{a,t,t+s}$. We assume that no adult survives past the age of A periods by setting $\Gamma_{a,t,t+s} = 0$ for $s > A - a$.

Households face the following sequence of budget constraints

$$C_{a+s,t+s} + n_{a+s,t+s}C^c_{a+s,t+s} + K_{a+s+1,t+s+1} = \left(K_{a+s,t+s} + \phi\Xi_{t+s}\right)\left(R^K_{t+s} + 1 - \delta\right) + e_{a+s,t+s}W_{t+s},$$

where $K_{a,t}$ is the age a adult's capital holdings at the beginning of the period, $e_{a,t}$ is the age a adult's labor endowment, R^K_t is the real rental rate of capital, and W_t is the real wage rate. We assume that only a fraction $\phi \in [0,1]$ of the capital held by adults who die, Ξ_t, at the beginning of the period is redistributed, with the remainder being lost. In short, the budget constraint states that family consumption and net investment (in capital units) cannot exceed the adult's income from renting her capital units (both previously saved and inherited) and supplying labor.

Optimality requires that consumption per dependent children net of the subsistence level be proportional to adult consumption net of the subsistence level,

$$\frac{C^c_{a+s,t+s} - Z_{t+s}\bar{C}^c}{C_{a+s,t+s} - Z_{t+s}\bar{C}} = \left(\epsilon n^{\eta-1}_{a+s,t+s}\right)^{\frac{1}{\nu}}.$$

The assumed utility function is flexible in that the factor of proportionality can be scaled by the parameter ϵ and can exhibit curvature in the number of children through the setting of η. This proportionality allows us to express the household objective function in terms of adult consumption

$$\sum_{s=0}^{A-a} \beta^s \Gamma_{a,t,t+s}\left(1 + \epsilon^{\frac{1}{\nu}}\left(n_{a+s,t+s}\right)^{1+\frac{\eta-1}{\nu}}\right)\frac{\left(C_{a+s,t+s} - Z_{t+s}\bar{C}\right)^{1-\nu}}{1-\nu} \tag{2}$$

[1] The existence of a subsistence level of consumption ensures that consumption will not counterfactually fall toward zero as adults in the model become very old. Moreover, the presence of labor-augmenting technology preserves consistency with balanced growth.

with a sequence of budget constraints given by

$$\left(1+\epsilon^{\frac{1}{\nu}}\left(n_{a+s,t+s}\right)^{1+\frac{\eta-1}{\nu}}\right)C_{a+s,t+s}-\epsilon^{\frac{1}{\nu}}\left(n_{a+s,t+s}\right)^{1+\frac{\eta-1}{\nu}}Z_{t+s}\bar{C}+n_{a+s,t+s}Z_{t+s}\bar{C}^{c}$$
$$+K_{a+s+1,t+s+1}=\left(K_{a+s,t+s}+\phi\Xi_{t+s}\right)\left(R_{t+s}^{K}+1-\delta\right)+e_{a+s,t+s}W_{t+s}.$$

We write the intertemporal Euler equation in terms of adult consumption as

$$\left(\frac{C_{a+1,t+1}-Z_{t+1}\bar{C}}{C_{a,t}-Z_{t}\bar{C}}\right)^{\nu}=\beta\Gamma_{a,t,t+1}\left(1+R_{t+1}^{K}-\delta\right). \tag{3}$$

The above equation illustrates how life-cycle elements affect the parent's consumption growth profile. In addition to the usual discount factor, β, the effective rate at which the household discounts the future depends on the probability of surviving to enjoy consumption in the next period. In the absence of a bequest motive, adults become increasingly impatient as they approach the end of life and the probability of dying rises. To the extent that the probability of surviving is close to 1 in the early decades of adulthood, consumption growth is fairly steady because the young are relatively patient. Consistent with this prediction, Browning and Ejrnæs (2009) provide evidence that two-adult households without children—for which household consumption roughly equals adult consumption—have fairly flat consumption profiles over their mid life.

The model also predicts that total household consumption, $C_{a,t}^{h}=C_{a,t}+n_{a,t}C_{a,t}^{c}$, will adjust to reflect changing family composition. As an illustration, assume temporarily that $\bar{C}=\bar{C}^{c}=0$, a restriction that is useful for exposition purposes. The objective function becomes

$$\sum_{s=a}^{A}\beta^{t+s-a}\Gamma_{a,t,t+s-a}\left(1+\epsilon^{\frac{1}{\nu}}\left(n_{s,t+s-a}\right)^{1+\frac{\eta-1}{\nu}}\right)^{\nu}\frac{\left(C_{s,t+s-a}^{h}\right)^{1-\nu}}{1-\nu}\equiv\sum_{s=a}^{A}\hat{\beta}_{a,t,t+s-1}^{t+s-a}\frac{\left(C_{s,t+s-a}^{h}\right)^{1-\nu}}{1-\nu}$$

where $\hat{\beta}_{a,t,t+s-1}^{t+s-a}$ can be interpreted as the effective rate at which the household discounts future consumption flows. The presence of children directly affects $\hat{\beta}_{a,t,t+s-1}^{t+s-a}$. When the number of children in the subsequent periods relatively high, the household acts as is if were relatively patient, which helps boost total household consumption in later periods. As we shall see, this mechanism helps produce hump-shaped consumption profiles over the life cycle. Additionally, the effect $n_{s,t+s-1}$ on $\hat{\beta}_{a,t,t+s-1}^{t+s-a}$ demonstrates how family composition directly affects the equilibrium real rate.

2.1.1 An alternative adult-equivalent specification

The predicted peak in household consumption in our baseline model occurs earlier in the life cycle than it does in the data. As an alternative, we consider a variant Browning and Ejrnæs' (2009) preferences in which total household consumption increases in the ages of the children. Accordingly, household utility is given by

$$\sum_{s=0}^{A-a} \beta^s \Gamma_{a,t,t+s} \frac{\left(C^h_{a+s,t+s} e^{-f_{a+s,t+s}} - Z_{t+s}\bar{C}\right)^{1-\nu}}{1-\nu} e^{f_{a+s,t+s}}, \tag{4}$$

where $\bar{C}$ is a subsistence level of consumption per adult equivalent family members. The function $f_{a,t} = \delta_h \ln(m_{a,t})$ allows for economies of scale in consumption based on the number of adult-equivalent members of the household, denoted $m_{a,t}$.[2] We compute the number of adult-equivalent members of the household as

$$m_{a,t} = 1 + \sum_{\sigma=0}^{A_c} n_{a,\sigma,t} g(\sigma),$$

where A_c is the maximum age before a dependent child becomes financially independent in the model and $n_{a,\sigma,t}$ is the number of children aged σ who are dependent from a representative adult aged a in period t. The function g captures how the age of the children translates into adult-equivalent household members. Similar to Browning and Ejrnæs (2009), we assume that

$$g(\sigma) = \mu_0 + \mu_1 \left(\frac{\sigma}{A_c}\right) + \mu_2 \left(\frac{\sigma}{A_c}\right)^2 + \mu_3 \left(\frac{\sigma}{A_c}\right)^3.$$

This function has $g(0) = \mu_0$ and our calibration will be such that it is increasing in σ. We further require that $\mu_3 = 1 - \mu_0 - \mu_1 - \mu_2$ so that $g(\sigma) \to 1$ as a dependent child approaches adulthood. Our appendix derives the equilibrium conditions under this specification of preferences.

2.2 Firms

The representative firm rents capital and labor inputs in perfectly competitive markets. It uses those factors in a Cobb-Douglas production function with labor-augmenting technology. The

[2] Although the utility function is specified in terms of total household consumption, we retain the dependence on the survival rate of adults. Current and projected mortality rates are rather low for the adult's child-rearing years, so that $\Gamma_{a,t,t+1}$ remains close to one until late in life when household consumptions coincides with adult consumption. This assumption is less innocuous for the early decades of the sample when life expectancy was appreciably shorter.

problem of the firm is to maximize profits net of factor costs,

$$K_t^{\alpha} \left(Z_t L_t\right)^{1-\alpha} - L_t W_t - R_t^K K_t,$$

taking factor prices as given. We assume that the firm's technology grows at a constant rate, $Z_t/Z_{t-1} = 1 + z$. At the optimal solution, the representative firm pays a rental rate on capital equal to the marginal product of capital,

$$R_t^K = \alpha \left(\frac{K_t}{Z_t L_t}\right)^{\alpha-1}, \tag{5}$$

and a real wage rate equal to the marginal product of labor,

$$\frac{W_t}{Z_t} = (1-\alpha) \left(\frac{K_t}{Z_t L_t}\right)^{\alpha}. \tag{6}$$

2.3 Aggregation, market clearing, and equilibrium

In our OG economy, the size of the population varies from period to period as new individuals are born and others die. Let $\mu_{s,t}$ be the number of individuals aged s at the beginning of period t after a new cohort of babies have been delivered but before deaths have occurred. Equilibrium in the labor market requires that

$$L_t = \sum_{s=A_c+1}^{A} \mu_{s,t} e_{s,t},$$

while equilibrium in the capital market requires

$$K_t = \sum_{s=A_c+1}^{A} \mu_{s,t} \Gamma_{s,t,t+1} K_{s,t} + \phi \sum_{s=A_c+1}^{A} \mu_{s,t} \left(1 - \Gamma_{s,t,t+1}\right) K_{s,t}.$$

The total capital stock is composed of two terms. The first term is the capital that surviving adults brought into the period. The second term is the redistributed capital from dead adults. Finally, goods-market clearing requires that production be equal to the sum of consumption and gross investment aggregated across the cohort-representative adults,

$$K_t^{\alpha} \left(Z_t L_t\right)^{1-\alpha} = \sum_{s=A_c+1}^{A} \mu_{s,t} \left(1 + \epsilon^{\frac{1}{\nu}} \left(n_{s,t}\right)^{1+\frac{\eta-1}{\nu}}\right) C_{s,t} + \sum_{s=A_c+1}^{A} \mu_{s,t} \left(K_{t+1,s} - (1-\delta)\left(K_{t,s} + \phi \Xi_t\right)\right).$$

In a perfect-foresight equilibrium, in each period, (a) goods and factor markets clear, (b) factor prices correspond to their marginal product, (c) the bequests received by surviving adults sum up to the capital held by adults who passed away at the beginning of the period (net of any destroyed capital), and (d) household optimality conditions are satisfied.

2.4 Solution method

Our solution method to find the perfect-foresight general equilibrium is described in the appendix. In short, we conjecture the paths of aggregate variables over the 1900–2400 period and solve the problem of the cohort-representative adults. The solution to this problem is conditional on the paths of all aggregate variables and on the household's demographic variables, namely the mortality and fertility rates conditional on age and birth cohort, and, for the early cohorts, the distribution of capital holdings at the turn of 1900. We next compute new paths for the aggregate objects by aggregating across the individual investment, saving, and labor supply decisions of the cohort-representative adults and by imposing the first-order conditions of the representative firms. If these paths differ from our initial guesses, then we update the paths and iterate one more time. Once we have reached numerical convergence, our search for the equilibrium stops. Because the equilibrium is conditional on an initial distribution of capital holdings and population at the turn of 1900, all aggregate objects, including the equilibrium real rate, depend on these distributions. However, as we argue in the appendix, 1900 is sufficiently far in the past that reasonable choices of the initial distributions have little influence on equilibrium outcomes in the post-war period. The solution method is sufficiently rapid that we solve the model at a quarterly frequency.

3 Calibration

We begin by presenting the data that we used to calibrate the demographic factors, which are distinctive elements of our study, and then turn to discussing our calibration of the remaining factors of the model.

3.1 Birth, employment, and mortality

The key demographic variables in our model are the employment rates by age and cohort, the mortality rates by age and cohort, the total number of births by period, and the average number of dependent children given the adult's ages and birth cohort. In addition, the simulation requires

the initialization of the population by age, the children-parent dependency structure, and capital holding by age and cohort at the turn of 1900 when our simulation begins. Throughout the paper, we assume that adults aged 18 years or more make all life-cycle decisions for themselves and their dependents. Once a child turns 18 years old, he or she begins life as a decision-maker.

Figure 3 illustrates the remarkable stability of the U.S. employment rate conditional on age [since the BLS began reporting these statistics by five-year age bins in 1967]. The figure masks offsetting changes in the composition of the U.S. workforce between gender: As women entered the labor force and gained employment, they made up for corresponding declines in male employment. In light of this stability, we assume that the labor supply conditional on age is constant over our entire sample period at its 2014 level.[3] Labor endowments are interpolated to all quarterly periods of life using cubic splines. The employment rates of people aged less than 18 years old are set to zero to conform with the model's treatment of dependent children.

Our mortality rates conditional on birth year and age are derived from an actuarial study conducted by Bell and Miller (2005) from the U.S. Social Security Administration. These projections cover every decade from 1900 to 2100. We primarily use Table 7 "Cohort Life Tables for the Social Security Area by Year of Birth and Sex" to obtain the mortality rates. While there are separate statistics provided for males and females, there are no corresponding mortality rates for the population as a whole. To obtain mortality rates for all genders, we assume that there are 3.5 percent more male births than female births, a proportion within the range of historical variation. Mortality rates by cohort and age are aggregated across genders in proportion to the number of surviving males and females up to the period. We interpolate mortality rates conditional on age and cohort within inter-census periods and age groups using cubic splines. In our applications, we assume that the mortality rates at the turn of 1900 prevailed in all earlier periods and, similarly, that the mortality rate at the turn of 2100 prevail in all subsequent periods.[4]

We use data from three sources to derive a quarterly series of births for the 1900–2400 period.

[3]The labor supply decision is interesting in its own right, but requires confronting distortions such as government retirement programs. For the purposes of our study, the remarkable constancy of labor supply decisions over time indicates that treating labor supply as exogenous is a good approximation for studying demographic effects in the medium to longer run.

[4]The cohort born in 1900 had a lower probability of death at all ages then persons born earlier in the 19th century. For example, the probability of dying at age 65 conditional on having survived to age 64 was 3.6 percent for the cohort of men born in 1900, whereas 4.2 percent of men who turned 65 years in 1900 died that year. The corresponding gap for women is similar, suggesting that the fall steady fall in mortality rates around that time was not primarily due to lingering consequences of the U.S. civil war.

The first source comprises yearly population estimates by years of age published by the Census Bureau for 1900 to 1979.[5] We detail below how we use information on the number of infants and childhood mortality to extract a series for live births. The second source is a monthly series of live births published by the National Center for Health Statistics (NCHS). The series starts in January 1972 and draws on the same data as the Census population estimates. The third source is the United Nations' *World Population Prospects (WPP): 2015 Revision*, which provides births estimates and projections by five-year periods from 1950 to 2100.

We first extract a yearly series for the number of births from 1900 to 1972 using the Census Bureau's yearly population estimates. These estimates provide the number of individuals alive as of July 1 of each year. In the population, births and deaths take place nearly continuously whereas, in our model, births and deaths take place at a specific point in our discrete time period. This latter feature means that population in the model differs depending on whether it is measured before or after births and deaths occur. However, because we use quarterly information on mortality rates to extract a series for births, the precise timing of population measurement is of limited consequence. We posit that births, deaths, and population measurement occur sequentially during the period. Consistent with these timing assumptions, we treat Census population estimates as of July 1 as if they correspond to the measure of the surviving population at the end of the second quarter of calendar years. Given that the calibration uses quarterly data, alternative timing assumptions with respect to births, deaths, and population measurement would have negligible consequences for our population and births estimates.

Let $POP_{[0,1),t}$ be the number of infants less than a year old estimated by Census at the end of period t. Let B_t be the number of births at the beginning of period t; consistent with the model, births take place before deaths during the period, so that newborns face a nonzero probability of not reaching period $t+1$. The number of infants less than a year old is the sum of surviving births in the current and previous three quarters,

$$POP_{[0,1),t} = \gamma_{0,t}B_t + \gamma_{1,t}\gamma_{0,t-1}B_{t-1} + \gamma_{2,t}\gamma_{1,t-1}\gamma_{0,t-2}B_{t-2} + \gamma_{3,t}\gamma_{2,t-1}\gamma_{1,t-2}\gamma_{0,t-3}B_{t-3}, \quad (7)$$

[5]The Census Bureau also publishes population estimates at either quarterly or monthly frequencies from 1980 onward. We do not use this information given that we have official monthly statistics on the number of births starting in January 1972.

where $\gamma_{i,j}$ are parameters governing the probability of survival. For simplicity, we temporarily assume that the number of births is constant over four-quarter intervals ending in the second quarter of each calendar year, that is, $B_t = B_{t-1} = B_{t-2} = B_{t-3}$. This identifying assumption is made for practical convenience: A smooth quarterly birth series based on yearly averages will be derived at a later stage. Under this assumption, we can extract a quarterly sequence $\{B_t\}_{t=1900:Q3}^{1979:Q2}$ from knowledge of mortality rates and the yearly Census estimates of the number of infants less than a year old. For the first half of 1900, we are missing estimates of quarterly mortality rates for 1899 that would be used to compute $B_{1900:Q1} = B_{1900:Q2}$ from the number of infants in the smoothed 1900 Census estimates. We simply posit that the mortality rates are the same, conditional on age, as those prevailing in the first quarter of 1900 (that is, $\gamma_{a,Q'} = \gamma_{a,1900:Q1}$ for $Q' < 1900{:}Q1$). Averaging quarterly observations for each calendar year, we finally obtain a series of annual birth estimates from 1900 to 1979.

For the 1972–2014 period, we get annual birth figures directly from NCHS.[6] As Figure 4 shows, annual NCHS estimates (the green diamonds) closely match the annual estimates that we derived above from mortality rates and infant population estimates (the blue stars) from 1972 to 1979 when the two samples overlap. We thus construct an annual births series from 1900 to 2014 by stitching the yearly figures derived from Census for 1900 to 1971 with those from NCHS for 1972 to 2014.

Finally, to obtain annual birth estimates after 2014 onward, we note that, in recent decades, yearly observations from the NOSH series (the green diamonds) essentially coincide with the corresponding five-year WPP data measured at the middle year (the blue circles). We thus allocate WPP data after 2009 to the mid-point of their five-year intervals through 2100, and stitch those five-year observations with the annual series through 2014. We then use cubic splines to extract quarterly birth estimates from 1900:Q2 to 2099:Q4. Of note, by the end of the current century, the WPP data project that live births have stabilized. Using this observation, we impose that the number of live births is constant from the last WPP data point (that is, 2097.5) through 2400. This assumption, along with constant mortality rates and no immigration, ensures the existence of a stable population distribution in the model over the long run.

[6] We could, in theory, use the monthly NCHS information to construct the quarterly estimates used in the model. Doing so would require removing apparent seasonal patterns.

3.2 Population at the turn of 1900

There are a number of caveats related to the initialization of the population worth mentioning. First, our model ignores immigration, which has varied over time in terms of importance and composition. In particular, detailed Census data indicate that young men are over-represented among immigrants. It can be difficult to ascertain when immigrants joined the resident population or what value one should attach to their labor endowments and asset holdings. Our model side-steps these questions by taking the population in the final quarter of 1899 as given and by then letting the population evolve according to the birth and mortality rate series derived above. Population growth due to immigration after 1900 will thus not be captured directly, although births from immigrant parents will nonetheless be included and help grow the population over time. Second, raw Census data are noisy, especially at the beginning of the sample period. For example, there are large spikes in the number of persons whose age in years ends with either a 0 or a 5, as the green stars in Figure 5 illustrate. This feature motivates us to work with smoothed population estimates.

Like our strategy to estimate births before the 1970s, our initialization of the population at the end of 1899 is based on estimates of the number of infants in smoothed population estimates provided by the Census Bureau along with our quarterly mortality rate estimates conditional on age and cohort. The 1900 smoothed Census population figures are being measured as of July 1, they must therefore be rolled back by two quarters. We again assume that all births take place at the beginning of the quarter, followed by deaths and then by population measurement. We assume that the number of births is constant over four-quarter periods ending in the second quarter of each calendar year. In the same way that we solved for B_t in equation 7, we can derive an estimate of the number of quarterly births consistent with the mortality rates as

$$\begin{aligned} B_{t-4a} &= POP_{[a,a+1),t} \Big/ \left(\gamma_{4(a-1)+1,t} \prod_{j=1}^{4(a-1)} \gamma_{j,t-1} + \gamma_{4(a-1)+2,t} \prod_{j=1}^{4(a-1)+1} \gamma_{j,t-1} \right. \\ &\quad \left. + \gamma_{4(a-1)+3,t} \prod_{j=1}^{4(a-1)+2} \gamma_{j,t-1} + \gamma_{4(a-1)+4,t} \prod_{j=1}^{4(a-1)+3} \gamma_{j,t-1} \right). \end{aligned}$$

One minor complication is that the smoothed yearly population estimates for 1900 subsume individuals ages " 75 years and over" into a single category. To estimate the population conditional

on age at a finer level of disaggregation for years 75 and above, we extrapolate the smoothed Census data using raw population counts from the 1900 U.S. Census, which are tabulated by year up to 99 years of age, and then have a "100 years and over category." To undo the presence of spikes around ages in years ending in 0s and 5s, we first fit a fourth-order polynomial on those yearly figures, then project them on a quarterly basis.[7] We then stitch the smoothed quarterly estimates for the quarters not covered by the historical population data. Finally, we run cubic splines on their yearly population figures at the end of 1899 to remove any residual seasonality. The resulting quarterly series is shown as the solid black line in figure 5, along with the Census Bureau's raw and smoothed population estimates for 1900.

3.3 Family composition

We obtain a measure of the number of dependent children per adult in two steps. We first estimate the number of births per mother of a given age. We then adjust the age of the mother by an estimate of the age difference between married men and women to obtain the age of the parents.

The main data source is a set of fertility tables published by Hamilton and Cosgrove (2010) from the Center for Disease Control (CDC). The tables provide estimates of the number of live births in each calendar year conditional on the age (in years) of the mother. They cover the 1917–1973 and 1960–2009 periods. The 1917–1973 figures have not been adjusted to the same extent by CDC staff for various sample adjustments/reporting errors. However, Figure 7 shows the share of births accruing to women of various age groups are fairly constant across the two samples. For 1917 to 1959, the figure depicts the shares from the 1917–1973 tables. From 1960 onward, the figure uses the share from the 1960 sample. Given that the shares are connected seamlessly at the 1960 stitching, we use the pre-1960 data without further adjustments.[8] We then extrapolate the data by quarter of life and quarter of the sample period using cubic splines. The Figure 6 below shows

[7] To ensure that the total number of persons aged 75 years and over in these smoothed projections coincides with the total number of persons aged 75 years and over in the U.S. Census' historical (that is, filtered) population estimates, we appropriately scale our smoothed quarterly population projections.

[8] By comparing the number of births by age of the mother over the samples' overlapping period (1960 to 1973), we note that the 1960-2009 sample corrects for underreporting of the number of births in the 1917-1973 samples. While the largest corrections are for mothers in their 20s. The adjustment factors for specific adjustments are quite choppy and volatile across years. The underreporting of live births in the 1973 is a key reason why we rely on smoothed Census population estimates to derive our series for live births in the early decades of the sample.

the share of births accruing to women for a number of age categories.

To compute the average age of the parent, we first impute the age gap between fathers and mothers using historical information on the median age of men and women at time of their first marriage. This information is available from 1890 through 2014. The historical data is based on decennial census information whereas the new data draw primarily from the Current Population Survey conducted by the Census Bureau, with adjustments made to line up with census information. While the age of first marriage has crept up over time for both women and men, Figure 7 shows that median age gap between men and women has been somewhat stable over the past several decades, at between 1.5 and 2.5 years.

We allocate children based on the average age of their parents, with the age of the mother taken from the CDC survey and the age of the father imputed by a smoothed version of the age difference between the median age of fathers and mothers at first marriage.[9] We first extend the Census/CPS data from 2015 through 2100 on an annual basis using the average age gap in 2013 and 2014. We then run a fifth-order polynomial through the resulting data points from 1890 to 2100. We use this polynomial fit for the 1900–2014 period. For the 2015–2100 period, we take a weighted average of the polynomial fit and the average age gap in 2013 and 2014. We gradually eliminate high-order dynamics by using triangular weights so that, by 2100, the fitted value equals the mean in 2013 and 2014. For 2100 onward, we keep the average age gap constant at its 2013–2014 average. Figure 7 shows the fitted values, which are very close throughout the period.

A question arises with teen pregnancies because young mothers may still be dependent children themselves. In the absence of detailed information, we follow a somewhat simple procedure. Whenever a child is born to parents whose average age is less than 18 years old, we allocate the child to her grandparents. Once the child's parents turn 18 years old, they become fully responsible for their child's consumption. With all the above information at hand, we can allocate children at the end of 1899 to their parents and calculate the average number of dependents entering the parents consumption function. We can then iteratively calculate the population and family structure over the full sample period by letting the population evolve according to births and deaths. Finally, we note that our procedure works only with averages rather than actual family cells. For

[9] To avoid small jumps in the allocation due to discrete nature of time in the model, births are allocated to nearby quarters in proportion of the distance from each.

example, deaths of adults and children do not result in discrete jumps in the number of dependents or surviving parents. Figure 8 shows the average number of dependent children by the age of their parents for a number of birth cohorts.

3.4 Other parameters of the model

The remainder of the parameters pertain to the representative adult's utility function and to the representative firm's production function. Our baseline calibration features no technology growth ($Z_t/Z_{t-1} = 1$) and no subsistence levels ($C = C^c = 0$). We set the elasticity of substitution in the utility function to unity ($\nu = 1$). For the version of the model in which the consumption of dependent children enters the utility of their parents through an additive terms, we follow Chadwick *et al.* (2015a, 2015b) in setting $\eta = 0.76$ and $\epsilon = 0.65$; the version of the model without dependent kids has $\epsilon = 0$. For the alternative specification of the utility function with adult-equivalent children, we adopt Browning and Ejrnæs' (2009) parameter estimates for educated families ($\eta = 0.921$, $\mu_0 = -0.266$, $\mu_1 = 2.847$, $\mu_2 = -6.119$, and $\mu_3 = 1 - \mu_0 - \mu_1 - \mu_2$). We set the share of capital in production, α, to 0.35, and the fraction of capital bequested, ϕ, to 1. The last parameter that we need to pin down is the household's discount factor. Unless otherwise indicated, we calibrate this parameter such that the average level of the real short-term rate in the 1980s matches the point estimate of Johannsen and Mertens (2016) for the period.

4 Results

We conduct two kinds of exercises to gauge the contribution of family structure and life expectancy to movements in the equilibrium real rate in recent and upcoming decades. We first calculate balanced growth path equilibriums under various calibrations of demographic variables, technology growth processes, and utility parameters. The exercise is designed to provide intuition about the effects of life-cycle factors on the equilibrium real rate over extended periods, and to illustrate how demographic variables influence the individual saving-investment decisions that ultimately drive the aggregate dynamics. We then use dynamic simulations of the model to extract historical paths of

the equilibrium real rate and other macroeconomic variables conditional on observed and projected U.S. demographic variables.

4.1 Balanced growth equilibrium

We begin by characterizing the balanced growth path of our model economy under the assumptions of no technology growth ($z = 0$) and no utility derived from child consumption ($\epsilon = 0$); we later relax both assumptions. We consider three baseline calibrations of the demographic variables. In the "1900 calibration," we assume that annual population growth is 1.9 percent—the average growth rate in the number of births between 1900 and 1905—and that the probability of dying every period is given by our interpolation of Bell and Miller's (2005) mortality tables conditional on age for individuals who were alive at the turn of 1900. Similarly, in the "2000 calibration" and "2100 calibration," we assume that the growth rate of the population matches our estimates of the growth rate of births in those years and we condition the survival probabilities on the mortality rate tables for individuals born in those years. Because the exercise is illustrative of how—all else equal—demographic variables and utility parameters affect the results, we impose that the discount factor is the same across all simulations shown in Figure 9.

4.1.1 Equilibrium real rate

The diamonds in the upper-left panel of Figure 9 show the equilibrium real rates as a function of the growth rate of the population for our three baseline calibrations. Differences in the level of the equilibrium real rate across balanced growth paths are economically large: The equilibrium real rate for 1900, at 2.3 percent, is more than two percentage points higher than the equilibrium real rate in the 2100 calibration, at 0.1 percent, a gap explained entirely by differing demographic characteristics. The equilibrium real rate for the 2000 calibration, at 0.7 percent, is closer to that in the 2100 calibration than to that in the 1900 calibration, suggesting that much of the decline in the equilibrium real rate between 1900 and 2100 reflects changes in demographic characteristics unfolding over the 20th Century.

The upper-left panel also offers some initial exploration of which life-cycle element—extended

life expectancy or lower population growth—is most important to explain realized and projected declines in the equilibrium real rate. To this effect, for all three baseline calibrations, we report the equilibrium real rate over a range of population growth holding constant all other parameters. As the baseline OG model in section 2.1 predicted, we find that the equilibrium real rate along the balanced growth path is increasing in the rate of population growth, with a one percentage point change in population growth being associated with a roughly $\frac{1}{4}$ percentage point movement in the equilibrium real rate under all three baseline calibrations. This somewhat modest change indicates that the largest contributor to the decline in the equilibrium real rate between our 1900 and 2100 calibrations is the fall in mortality rates, which greatly increases the number of years one expects to depend primarily on accumulated savings to fund consumption, and thus incentivizes saving ahead of retirement.

The remaining panels of Figure 9 show the effects assuming that technology growth is strictly positive, that parents derive utility from their dependent children's consumption, or both. Starting with higher technology growth, the upper-right panel shows that raising technology growth from zero to 1.25 percent per year boosts the level of the equilibrium real rate in all three baseline calibrations of the balanced growth path. The effect is roughly uniform across calibrations and rates of population growth, consistent with nearly full pass-through of higher technology growth to the equilibrium real rates. For example, the equilibrium real rate in the 2000 calibration rises from 0.76 percent to 1.81 percent, an increase of 1.05 percentage points.

Factoring the consumption of dependent children into the utility function of the cohort-representative adults similarly raises the equilibrium real rate (lower-left panel). Whereas higher rates of productivity growth directly boost the marginal product of capital, the presence of dependents makes it harder for adults to accumulate capital, so that the scarcity of capital relative to labor boosts the returns on each unit invested. The bottom-right panel shows a combination of both higher technology growth and the presence of dependents, in which the effects of these two factors on the equilibrium real rate combine in a nearly additive way.

Although the particular level of interest rates is sensitive to our assumptions about technology growth and the utility function, three key findings are robust across the four panels. First, the predicted fall in the equilibrium real rate over the 1900 and 2100 calibrations is economically large, at roughly 2 percentage points. Second, both lower population growth and longer life expectancies

contribute to the decline, with longer life expectancy being the largest contributor. Finally, at least half of the decline in the equilibrium real rate reflects changes in demographic factors unfolding over the 20th century. As we will show below, these conclusions will also apply to the dynamic version of the model.

4.1.2 Individual consumption and saving decisions

Figure 10 illustrates the individual consumption/saving decisions of adults at various points in their life under the 2000 calibration, both with and without the consumption of children entering their parents' utility. By assumption, agents in the model start adulthood with no accumulated capital and thus initially can only rely on their labor income, inheritances, and borrowing to fund consumption. In the specification with no dependents, young adults anticipate that their labor endowment—and hence their period income—will grow in the future. Their desire to smooth consumption is such that they initially borrow to fund a fraction of their consumption. Adult consumption rises gently until the adults 50s because the economy's equilibrium real rate slightly exceeds the adults effective discount rate. From the adult's 60s onward, the increasing probability of death increases the rate at which adults discount future consumption, leading them to run down their stock of assets. In fact, relatively high effective discount rates encourage older adults to borrow against their future consumption.[10] By the time adults reach their late 90s, consumption approaches zero. As is well known, the empirical evidence showing that consumption steps down as the adult enters retirement conflicts with the strong consumption smoothing motives in the model. Similarly, the running down of asset conflicts with evidence that, on average, retired adults are reluctant to drive down their asset holdings to near zero.[11]

The assumption that adults derive utility from their dependent children has a marked effect on their consumption/saving decisions. The anticipation that consumption will be limited by that of their children incentivizes young adults to save early on, dampening the initial rise in consumption at the turn of the 20s. As the number of dependent children rises toward its peak in the adult's 20s

[10] We assume that adults live off their net savings and inheritance income in the last period of their existence. Combined with the condition that consumption be strictly positive, this end-of-life creates an effective borrowing constraint that prevents capital holdings from falling much below zero.

[11] We plan to explore the effects on the equilibrium real rate of standard fixes to these counterfactual predictions, such as the introduction of bequest motives or uninsurable idiosyncratic risk, in future work.

and 30s, the accumulation of capital slows appreciably to allocation family resources to children consumption. Eventually, the number of dependent children begins to fall and adults can resume building their asset holdings at a higher rate. Adults' asset holdings peak in their mid-60s, and then starts falling as they seek to maintain consumption in the face of a dwindling labor income and as their increasing mortality rate effectively makes them less patient.

At a qualitative level, the prediction that households with no kids have consumption profiles that are rather flat (the blue line in the top panel) whereas those with kids have consumption profiles that are hump shaped (the dashed red line) accords with the empirical evidence presented in Browning and Ejrnæs (2009). The timing of the peak in total household consumption occurs somewhat earlier than in the data under our baseline utility function. As a robustness exercise, we adopt the alternative adult-equivalent specification estimated by Browning and Ejrnæs (2009), which allows for the consumption needs of children to rise with their age, thus postponing the peak in total household consumption relative to our baseline utility specification. These authors show that their alternative utility calibration captures U.S. prime-age consumption-saving dynamics without recourse to other frictions (at least for the recent period for which such data are available). However, as we will show, the effects of demographics on the equilibrium real rate, which is the focus of our inquiry, are essentially the same as under our baseline calibration.

4.2 Dynamic equilibrium

Our dynamic simulations track the evolution of the U.S. economy from 1900 to 2100. However, our discussion focuses on the implications of the U.S. demographic transition for the recent and next few decades. One reason to discount the results in the early decades of the sample is that the initialization of the simulation is subject to much uncertainty. The beginning of our sample was only 35 years after the end of the U.S. Civil War, which saw the destruction of a substantial amount of capital and the tragic loss of life of about 2.5 percent of the population—essentially young men who would have been part of the working-age population in subsequent decades. Moreover, as we noted in section 3.2, the 1900 census statistics are rather imprecise.[12] Similarly, one reason to discount

[12]Section 3.2 notes that raw Census population data in 1900 display jumps in the number of persons reporting that their age in years ends with either a zero or a 5. Also, the number of infants in the 1900 Census appears to be somewhat underestimated relative to what would be expected by the high infant mortality rate estimates of Bell and

the results in future decades is that demographic projections become increasingly uncertain the farther one goes into the future.

4.2.1 Equilibrium real rate since the 1960s

The top panel of Figure 11 shows the model's equilibrium real rate over the 1960–2030 period under our baseline specification of the utility function, for which the consumption of dependent kids does not enter their parents' utility (the solid blue line). At a qualitative level, the model generates a path of the equilibrium real rate that resembles the path of Johannsen and Mertens' (2016) point estimates: the equilibrium real rate increases through most of the 1960s and 1970s, reaching a peak in the 1980s, and then steadily falling thereafter. At a quantitative level, Johannsen and Mertens (2016) estimate that the equilibrium real rate has fallen $\frac{3}{4}$ percentage point since the 1980s. Our model predicts an equally large fall, only over a slightly longer period. There is admittedly much uncertainty attached to any time-series estimate of the equilibrium real rate, as the uncertainty bands in the panel highlight. Nevertheless, we see the remarkable similarity in the timing of the rise, peak, and decline of the equilibrium real rate, along with similar magnitudes of decline since the 1980s, as indicating that the model's predictions are largely consistent with the time series evidence. Put differently, demographic factors appear to be an economically important contributor to low-frequency movements in the equilibrium real rate, explaining possibly most if not all of the permanent decline in recent decades.

The results are broadly similar when we assume that children consumption enters the parents' utility function (the solid green line), with one notable difference: When dependents are taken into account, the fall in the equilibrium real rate since the 1980s occurs initially slowly but then speeds up over the past decade or so. The Great Recession and its aftermath thus correspond to a period in which the equilibrium real rate is falling rapidly. As the bottom panel of Figure 11 shows, the results are essentially unchanged when we adopt our alternative adult-equivalent preferences.

Figure 12 provides further information about the effects of family and life expectancy on aggregate variables. By construction, the real rental rate of capital in our model mimics movements

Miller (2005), which we use throughout the sample period. Thankfully, however, the quality of the sample appears to have improved quickly, making us confident that our key findings are insensitive to reasonable deviations from the initialization of demographic data.

in the equilibrium real rate. The real wage measured in efficiency units falls through most of the 1960s and 1970s, reaching a trough in the 1980s, before steadily rising. These movements reflect the relative scarcity of factors of production. As the bottom-left panel shows, the number of dependent children dropped precipitously as U.S. baby boomers entered the labor force. The arrival of this large cohort of workers made labor relatively abundant, leading to a rise in the rental rate of capital relative to wages. However, as decades passed, the cohort of baby boomers amassed wealth ahead of its retirement. The bottom-left panel also shows that the number of inactive adults—that is, the average time endowment not spent working—relative to the employment rate reached a turning point over the past decades and will increase at a rapid pace over the next two decades as hordes of baby boomers retire.[13] Finally, the bottom-right panel shows that the movements in labor-force participation implied by the model. Labor-force participation rose from 1980 through the early 2000's, and then began falling as the baby-boom generation began to retire.

The figure also shows that there is not a direct mapping between the real rate and the net saving (investment) rate, which we measure as the net change in the capital stock relative to GDP.[14] Even though the net saving rate is currently declining, the model predicts that the equilibrium real rate is falling because capital-labor ratio is increasing. This observation cautions that simple dynamic analysis that ignore the rich variation in demographic factors and composition of the population might draw incorrect conclusions. Moreover, it suggests that demographic factors might offer a complementary explanation for seemingly weak business investment in the wake of the Great Recession, which some authors have traced back to persistent restrictions on the cost and availability of credit and to limited investment opportunities in the face of depressed demand.

4.2.2 Counterfactual scenario: constant mortality rates

To assess the respective contributions of longer life expectancy and lower population growth on the fall in the equilibrium real rate since the 1980s, we perform an alternative simulation in which we assume that the mortality rates at the end of the 1950s prevail over all subsequent periods.[15] As

[13] This ratio is given as $(1 - e_t)/e_t$, where e_t is the average employment rate of adults in the sample.

[14] That is, we define net saving as $\frac{K_{t+1} - K_t}{(K_t)^{\alpha}(Z_t L_t)^{1-\alpha}}$.

[15] Put differently, a person aged a in periods after 1959:Q4 faces the same mortality rate as someone aged a in 1959:Q9 did at the time.

with our other dynamic simulations, we recalibrate the discount factor such that the model matches Johannsen and Mertens (2016) average estimate in the 1980s of the real interest rate in the long-run. We present the counterfactual path of the equilibrium real rate in figure 13. Holding mortality rates constant has been modest: The fall in the equilibrium real rate since the 1980s is estimated to be only about 15 basis points smaller when we fixed the mortality rates to their 1959:Q4 levels than when we let mortality rates follow their historical paths. Thus, whereas the extension of life expectancy was the main driver of the difference in the equilibrium real rate between our 1900 and 2100 balanced growth calibration, the fall in the equilibrium real rate since the 1980s is dominated by dynamics associated with changes in cohort sizes.

That changes in life expectancy alone have had only a small effect on the equilibrium real rate since the 1980s is perhaps unsurprising. To put these changes in mortality rates in perspective, we note that the mean life expectancy at birth conditional on the mortality rates observed at the turn of 1980, at 79.6 years, was only three and half years less than the corresponding statistic based on the mortality rates prevailing in 2015. By contrast, the total gain in life expectancy over the 1900–2100 period is nearly three and a half decades. Moreover, the gains in life expectancy over the past few decades reflect primarily a fall in mortality rates during an adult's years in retirement, and thus have almost no effect on the aggregate supply of labor. And with younger cohorts discounting the consumption of their older selves, the incentive to accumulate more capital in the early productive years are little changed. On net, the aggregate stock of capital rises only modestly and the fall in the equilibrium real rate is accordingly small.

4.3 Open economy considerations

We next turn to the predictions of our model over extended horizons. In a related multi-country set up with migration and free capital movements, Kruger and Ludwig (2007) find a decline in the U.S. real rate of return of 86 basis points from 2005 to 2080 (or 79 basis points if the United States were a closed economy). Under the baseline version of our model with no dependent children, the natural rate of interest falls from 1.27 percent in 2005 to 0.60 percent by 2080, a difference of 67 basis points. Under the version of our model with dependent children, the drop is from 1.52

percent to 0.53 percent, a difference of 99 basis points.[16] The difference in the predicted extent of the fall over the 2005–2080 period between the tow versions of our model thus primarily reflects the demographic forces that led to a faster fall in real interest rates in recent years. Our range of estimates narrowly encompasses the estimates of Kruger and Ludwig (2007); accordingly, we see our findings as largely consistent with theirs, even though the specifics of our respective models differ.

Whereas our model has a richer family structure than that of Kruger and Ludwig (2007), their model accounts for open-economy influences whereas our model does not. This latter factor is potentially important factor for understanding the behavior of U.S. real interest rates. Notably, several authors have documented the strong correlation between real interest rates worldwide.[17] In a similar vein, Bernanke's (2005) global saving glut hypothesis challenged the idea that the dynamics of the U.S. current account since the mid-1990 reflected primarily domestic developments, pointing instead to global influences on interest rates such as an increased desire to save by emerging market economies in the wake of financial crises in the mid to late 1990s. By design, our model aims at explaining low-frequency movements in interest rates, and is thus not suited to explain saving behavior around crises episodes in which global factors may play an important but ultimately transitory role.

That said, in Kruger and Ludwig (2007), the magnitude of the projected effects of demographic factors are rather similar between the open-economy and close-economy version of their model. The reason is that the United States and the world's other advanced economies are undergoing demographic transitions that are similar in terms of magnitude and timing, so that global channels have a somewhat limited importance. In the top panel of figure 14, we show that the step down in U.S. working-age population growth unfolding since the 1970s echoes a similar pattern in OECD economies and in the world more broadly. In particular, the 2000–2030 period features an especially sharp slowdown in population growth. In the bottom panel, we show that the U.S. mean life expectancy at birth has been rising in tandem with that in the OECD economies. A similar gain in mean life expectancy at birth is observed when we include both developed and developing economies,

[16]The version of the model with adult-equivalent preferences predicts a drop from 1.53 percent in 2005 to 0.65 percent in 2080.

[17]On the correlation in real interest rates across countries, see, among many contributors, Desroches and Francis (2006), King and Low (2014), and Barro and Sala-i-Martin (1990).

although the level is pulled down by still markedly higher death rates in the less-developed countries. For all these reasons, we think demographic factors would likely prove economically important for understanding the behavior of the equilibrium real rate in a more general open-economy setting (see, for example, Banerjee *et al.* (2015)).[18]

5 Conclusion

In this paper, we used a calibrated OG model with a rich demographic structure to investigate the extent to which past and projected changed in U.S. family composition and life expectancy have had an influence on real interest rates and other variables. We find that demographic transitions alone account for a nearly $\frac{3}{4}$-percentage-point decline in the natural rate of interest since the 1980s—a magnitude that we argue is in-line with empirical estimates. We demonstrated that modeling the family structure is important for capturing the timing of that decline. In particular, calibrations with dependent children point to the real rates falling especially rapidly in recent and coming years, which suggests a risk that the permanent effects of demographic factors could be misinterpreted as persistent but ultimately transitory downward pressure on the natural rate of interest and net savings stemming from the Great Recession. Furthermore, we use the model to demonstrate that demographic changes have been, and will continue to be, a drag on real business investment, which have also been described as abnormally low in the wake of the Great Recession. And with the equilibrium real rate predicted to fall below 1 percent within the next decade, and to continue to fall thereafter, our analysis suggests that low real interest rates are part of the new economic reality.

[18] Unfortunately, the availability of historical demographic data and their projected trends is typically more limited in most countries than in the United States. This situation renders impossible the extension to the global economy of an OG framework with a demographic structure as rich as ours.

References

[1] Attanasio, Orazio, Sagiri Kitao, and Giovanni L. Violante (2007). "Global demographic trends and social security reform," *Journal of Monetary Economics*, vol. 54(1), pages 144–198.

[2] Banerjee, Ryan Niladri, Jonathan Kearns, and Marco Jacopo Lombardi (2015). "(Why) Is investment weak?," *BIS Quarterly Review*, Bank for International Settlements, March.

[3] Barro, Robert J. and Xavier Sala-i-Martin (1990). "World Real Interest Rates," NBER Chapters, in: *NBER Macroeconomics Annual 1990*, Volume 5, pages 15–74 National Bureau of Economic Research, Inc.

[4] Bell, Felicitie C. and Michael L. Miller (2005). "Life Tables for the United States Social Security, 1900-2100," Actuarial Study No. 120, Social Security Administration – Office of the Chief Actuary.

[5] Bernanke, Ben S. (2005). "The Global Saving Glut and the U.S. Current Account Deficit", speech delivered at the Sandridge Lecture of the Virginia Association of Economists, Richmond VA, March 10.

[6] Blanchard, Olivier Jean and Stanley Fischer (1989). *Lectures on Macroeconomics*, The MIT Press, Cambridge, MA.

[7] Browning, Martin and Mette Ejrnæs (2009). "Consumption and Children," *The Review of Economics and Statistics*, vol. 91(1), pages 93–111.

[8] Carvalho, Carlos and Andrea Ferrero (2014). "What Explains Japan's Persistent Deflation?," mimeo.

[9] Carvalho, Carlos, Andrea Ferrero, and Fernanda Nechio (forthcoming). "Demographics and Real Interest Rates: Inspecting the Mechanism," *European Economic Review*, special issue on The Post-Crisis Slump.

[10] Curtis, Chadwick C., Steven Lugauer, and Nelson C. Mark (2015a). "Demographic Patterns and Household Saving in China," *American Economic Journal: Macroeconomics*, vol. 7(2), pages 58–94.

[11] Curtis, Chadwick C., Steven Lugauer, and Nelson C. Mark (2015b). "Demographics and Aggregate Household Saving in Japan, China, and India," NBER Working Papers 21555, National Bureau of Economic Research, Inc.

[12] Desroches, Brigitte and Michael Francis (2006). "Global Savings, Investment, and World Real Interest Rates," Bank of Canada Review, Bank of Canada, vol. 2006(Winter), pages 3–17.

[13] Eggertsson, Gauti B. and Neil R. Mehrotra, 2014. "A Model of Secular Stagnation," NBER Working Papers 20574, National Bureau of Economic Research, Inc.

[14] Favero, Carlo A., Arie E. Gozluklu, and Haoxi Yang (2014). "Demographics and the Behavior of Interest Rates," Working Papers wpn13-10, Innocenzo Gasparini Institute for Economic Research, Bocconi University.

[15] Hamilton, Brady E. and Cosgrove Candace M. (2010). "Central Birth Rates by Live-Birth Order, Current Age, and Race of Women in Each Cohort from 1911 through 1991: United States, 1960–2005. Table 1." Hyattsville, MD: National Center for Health Statistics. Available from: /nchs/nvss/cohort_fertility_tables.htm. Released: June 30, 2010.

[16] Ikeda, Daisuke and Masashi Saito (2014). "The effects of demographic changes on the real interest rate in Japan," *Japan and the World Economy*, vol. 32(C), pages 37–48.

[17] Johannsen, Benjamin K. and Elmar Mertens (2016a). "The Expected Real Interest Rate in the Long Run: Time Series Evidence with the Effective Lower Bound," FEDS Notes, Federal Reserve Board of Governors, February 9.

[18] Johannsen, Benjamin K. and Elmar Mertens (2016b). "Time Series Model of Interest Rates With the Effective Lower Bound," Finance and Economics Discussion Series 2016-033. Washington: Board of Governors of the Federal Reserve System.

[19] King, Mervyn and David Low (2014). "Measuring the 'World' Real Interest Rate," NBER Working Paper No. 19887, National Bureau of Economic Research, Inc.

[20] Krueger, Dirk and Alexander Ludwig (2007). "On the Consequences of Demographic Change for Rates of Returns to Capital, and the Distribution of Wealth and Welfare," *Journal of Monetary Economics*, vol. 54(1), pages 49–87.

[21] Rachel, Lukasz and Thomas Smith (2015). "Secular drivers of the global real interest rate," Bank of England working papers 571, Bank of England.

[22] McGrattan, Ellen R. (2012). "Capital Taxation During the U.S. Great Depression," *The Quarterly Journal of Economics*, vol. 127(3), pages 1515–1550.

[23] Mertens, Elmar and James M Nason (2015). "Inflation and Professional Forecast Dynamics: An Evaluation of Stickiness, Persistence, and Volatility," CAMA Working Papers 2015-06, Centre for Applied Macroeconomic Analysis, Crawford School of Public Policy, The Australian National University.

[24] Rogoff, Kenneth (2015). "Debt Supercycle, Not Secular Stagnation," Vox: CEPR's Policy Portal, April 22. At: http://www.voxeu.org/article/debt-supercycle-not-secular-stagnation.

[25] Yellen, Janet L. (2015). "The Economic Outlook and Monetary Policy," speech delivered at The Economic Club of Washington, Washington, D.C., December 2.

A Appendix: Solution method

A.1 General description of our algorithm

We follow an iterative procedure to compute an equilibrium in which (a) cohort-representative adults and the representative firm optimize conditional aggregate variables and demographic factors and (b) aggregate objects are consistent with the aggregation of individual decisions across adults and firms. This equilibrium is conditional on the path of the parameters of the model, the demographic variables, and initial distributions of the population and capital holdings. The steps in the procedure are as follows:

1. Compute two balanced growth equilibriums to the model. The first such equilibrium is parametrized to demographic data at the turn of 1900. It is used to obtain a reasonable distribution of capital holdings by age in the initial period. The second such equilibrium is parametrized to the demographic data assumed to prevail after 2100, and corresponds to the balanced growth path toward which the economy ultimately converges.

2. Compute the exogenous path of the labor supply by aggregating the labor endowments across adults.

3. Guess the path $R^{(0)} = \left\{R_t^{(0)}\right\}_{t=1900:Q1}^{T}$ and other aggregate objects, where T is a period sufficiently far into the future (in our case, 2399:Q4) that the economy has essentially converged back to its long-run balanced growth path. As a simple way to initialize $R^{(0)}$, we use a linear interpolation of the 1900 and 2100 balanced growth equilibrium values computed in the step above. We then project the 2100 values through the end of the simulation period. We initialize the paths of all other aggregate objects, such as bequests, factor prices, etc., using similar linear interpolations.

4. Given the paths of the aggregate objects and initial distribution of capital holdings, solve the problem of the cohort-representative adults who were alive at the turn of 1900. Then, solve the problem of each cohort-representative adult entering adulthood in subsequent periods.

5. Aggregate the individual decisions of firms and cohort-representative adults period by period to compute new paths of the aggregate objects, including for $\tilde{R}^{(0)}$.

6. Calculate the Euclidian distance between the two interest rate paths. If $\left\|\tilde{R}^{(0)} - R^{(0)}\right\| < \varepsilon$, where ε is positive but sufficiently small to claim numerical convergence, then you have found a numerical solution. If $\left\|\tilde{R}^{(0)} - R^{(0)}\right\| \geq \varepsilon$, then update the interest rate path using

$$R^{(0)} = \omega \tilde{R}^{(0)} + (1 - \omega) R^{(0)},$$

where $\omega \in (0, 1]$. Similarly update the paths of other aggregate objects, then return to step 4.

In our main results, we select the discount factor (that is, β) such the model's average equilibrium real rate in the 1980s coincides with the corresponding estimate from Johannsen and Mertens (2016). We implement the search for this discount factor using a bisection method.

A.2 Solving the problem of the cohort-representative adult

The most computing intensive element is step 4 because it requires solving each cohort-representative adult's life-cycle problem. The computation of a solution is made simpler by two sets of assumptions. First, problem is solved under perfect foresight of demographic and aggregate variables. Second, as we show below, the problem of the adult is linear in leads and lags of her capital holdings conditional on the paths of the aggregate objects and demographics. This linearity allows us to use linear algebra techniques to quickly derive a solution. Before we do so, we scale the equilibrium objects so that we have a stationary equilibrium along the balanced growth path.

Let the generic variable $\tilde{X}_t = X_t / Z_t$, where Z_t is labor augmenting technology. We begin by scaling the representative firm' optimal conditions (equations 5 and 6) that relate the real rental rate of capital to its marginal product,

$$R_t = \alpha \left(\frac{\tilde{K}_t}{L} \right)^{\alpha - 1},$$

and the real wage rate to the marginal product of labor,

$$\tilde{W}_t = (1 - \alpha) \left(\frac{\tilde{K}_t}{L} \right)^{\alpha}.$$

The intertemporal Euler equation is

$$\frac{\tilde{C}_{a+1,t+1}-\bar{C}}{\tilde{C}_{a,t}-\bar{C}}=\left(\beta\Gamma_{a,t,t+1}\right)^{\frac{1}{\nu}}\left(R_{t+1}+1-\delta\right)^{\frac{1}{\nu}}\left(\frac{Z_t}{Z_{t+1}}\right).$$

and the scaled budget constraint is

$$\left(1+\epsilon^{\frac{1}{\nu}}\left(n_{a,t}\right)^{1+\frac{\eta-1}{\nu}}\right)\tilde{C}_{a,t}-\epsilon^{\frac{1}{\nu}}\left(n_{a,t}\right)^{1+\frac{\eta-1}{\nu}}\bar{C}+n_{a,t}\bar{C}^{c}+\frac{Z_{t+1}}{Z_t}\tilde{K}_{a+1,t+1}=\left(\tilde{K}_{a,t}+\phi\tilde{\Xi}_t\right)\left(R_t+1-\delta\right)+e_{a,t}\tilde{W}_t.$$

Replacing the consumption terms in the intertemporal Euler equation, we get,

$$\begin{aligned}-\frac{Z_{t+2}}{Z_{t+1}}\tilde{K}_{a+2,t+2}+\left(R_{t+1}+1-\delta+\Omega_{a+1,t+1}\frac{Z_{t+1}}{Z_t}\right)\tilde{K}_{a+1,t+1}-\Omega_{a+1,t+1}\left(R_t+1-\delta\right)\tilde{K}_{a,t}\\ =\Omega_{a+1,t+1}\phi\left(R_t+1-\delta\right)\tilde{\Xi}_t-\phi\left(R_{t+1}+1-\delta\right)\tilde{\Xi}_{t+1}\\ +\left(1-\Omega_{a+1,t+1}\right)\left(\bar{C}+n_{a,t}\bar{C}^{c}\right)+\Omega_{a+1,t+1}e_{a,t}\tilde{W}_t-e_{a+1,t+1}\tilde{W}_{t+1},\end{aligned}$$

where

$$\Omega_{a+1,t+1}\equiv\left(\beta\Gamma_{a,t,t+1}\right)^{\frac{1}{\nu}}\left(R_{t+1}+1-\delta\right)^{\frac{1}{\nu}}\left(\frac{1+\epsilon^{\frac{1}{\nu}}\left(n_{a+1,t+1}\right)^{1+\frac{\eta-1}{\nu}}}{1+\epsilon^{\frac{1}{\nu}}\left(n_{a,t}\right)^{1+\frac{\eta-1}{\nu}}}\right)\left(\frac{Z_t}{Z_{t+1}}\right).$$

We note that the above expression is linear in the leads and lags of individual capital holdings conditional on aggregate variables and demographic factors. This observation allows us to express the equilibrium conditions of a cohort-representative adult aged a in period t as a system of linear equations, $\mathbf{M}\left(a,t\right)\tilde{\mathbf{K}}\left(a,t\right)=\mathbf{\Psi}\left(a,t\right)$. The vector of length $\left(A-a\right)$ containing the scaled capital holdings of the representative adult is

$$\tilde{\mathbf{K}}\left(a,t\right)=\begin{bmatrix}\tilde{K}_{a+1,t+1}\\ \tilde{K}_{a+2,t+2}\\ ...\\ \tilde{K}_{A-1,t+A-a-1}\\ \tilde{K}_{A,t+A-a}\end{bmatrix}.$$

The entries of the squared matrix $\mathbf{M}(a,t) = [m_{i,j}(a,t)]$ are

$$m_{i,j}(a,t) = \begin{cases} R_{t+j} + 1 - \delta + \Omega_{a+j,t+j}\left(\frac{Z_{t+j}}{Z_{t+j-1}}\right) & \text{if } j = i \\ -\Omega_{a+j+1,t+j+1}\left(R_{t+j} + 1 - \delta\right) & \text{if } j = i+1 \\ \frac{Z_{t+j+1}}{Z_{t+j}} & \text{if } j = i-1 \\ 0 & \text{otherwise.} \end{cases}$$

The elements of the vector $\mathbf{\Psi}(a,t) = [\psi_j(a,t)]$ are

$$\psi_j(a,t) = \begin{cases} \begin{array}{c} \Omega_{a+1,t+1} e_{a,t} \tilde{W}_t - e_{a+1,t+1}\tilde{W}_{t+1} \\ +\Omega_{a+1,t+1}\left(R_t + 1 - \delta\right)\phi\tilde{\Xi}_t - \left(R_{t+1} + 1 - \delta\right)\phi\tilde{\Xi}_{t+1} \\ +\left(1 - \Omega_{a+1,t+1}\right)\left(\bar{C} + n_{a+1,t+1}\bar{C}^c\right) \\ +\Omega_{a+1,t+1}\left(R_t + 1 - \delta\right)\tilde{K}_{a,t} \end{array} & \text{if } j = 1 \\ \begin{array}{c} \Omega_{a+j,t+j} e_{a+j-1,t+j-1} \tilde{W}_{t+j-1} - e_{a+j,t+j}\tilde{W}_{t+j} \\ +\Omega_{a+j,t+j}\left(R_{t+j-1} + 1 - \delta\right)\phi\tilde{\Xi}_{t+j-1} - \left(R_{t+j} + 1 - \delta\right)\phi\tilde{\Xi}_{t+j} \\ +\left(1 - \Omega_{a+j,t+j}\right)\left(\bar{C} + n_{a+1,t+1}\bar{C}^c\right) \end{array} & \text{if } 1 < j \leq A - a \end{cases}.$$

A.3 Equilibrium conditions under alternative adult-equivalent specification

The objective is to maximize equation 4 subject to

$$C^h_{a+s,t+s} + K_{a+s+1,t+s+1} = \left(K_{a+s,t+s} + \phi\Xi_{t+s}\right)\left(R_{t+s} + 1 - \delta\right) + e_{a+s,t+s}W_{t+s}.$$

We can write the Lagrangian as

$$\mathcal{L} = \sum_{s=0}^{A-a} \beta^s \Gamma_{a,t,t+s} \Bigg\{ \frac{\left(C^h_{a+s,t+s} e^{-f_{a+s,t+s}} - Z_{t+s}\bar{C}\right)^{1-\nu}}{1-\nu} e^{f_{a+s,t+s}} - \lambda_{t+s}\Big(C^h_{a+s,t+s} + K_{a+s+1,t+s+1} - \left(K_{a+s,t+s} + \phi\Xi_{t+s}\right)\left(R_{t+s} + 1 - \delta\right) - e_{a+s,t+s}W_{t+s}\Big)\Bigg\}.$$

Optimization requires

$$\frac{\tilde{C}^h_{a+1,t+1} e^{-f_{a+1,t+1}} - \bar{C}}{\tilde{C}^h_{a,t} e^{-f_{a,t}} - \bar{C}} = \left(\beta\Gamma_{a,t,t+1}\right)^{\frac{1}{\nu}}\left(R_{t+1} + 1 - \delta\right)^{\frac{1}{\nu}}\left(\frac{Z_t}{Z_{t+1}}\right) \equiv \Omega_{a+1,t+1},$$

where we have scaled the variables. Scaling the budget constraint and replacing consumption, we get

$$
\begin{aligned}
-\Omega_{a+1,t+1}e^{-f_{a,t}}\left(R_t+1-\delta\right)\tilde{K}_{a,t}+\left(\left(R_{t+1}+1-\delta\right)e^{-f_{a+1,t+1}}+\Omega_{a+1,t+1}e^{-f_{a,t}}\frac{Z_{t+1}}{Z_t}\right)\tilde{K}_{a+1,t+1}\\
-\frac{Z_{t+2}}{Z_{t+1}}e^{-f_{a+1,t+1}}\tilde{K}_{a+2,t+2}=\Omega_{a+1,t+1}\left(R_t+1-\delta\right)e^{-f_{a,t}}\phi\tilde{\Xi}_t-\left(R_{t+1}+1-\delta\right)e^{-f_{a+1,t+1}}\phi\tilde{\Xi}_{t+1}\\
+\Omega_{a+1,t+1}e^{-f_{a,t}}e_{a,t}\tilde{W}_t-e_{a+1,t+1}e^{-f_{a+1,t+1}}\tilde{W}_{t+1}+\left(1-\Omega_{a+1,t+1}\right)\bar{C}
\end{aligned}
$$

The solution to the cohort-representative household continues to be represented by a linear system of equations, $\mathbf{M}\left(a,t\right)\tilde{\mathbf{K}}\left(a,t\right)=\mathbf{\Psi}\left(a,t\right)$. The elements of the $\left(S-a\right)\times\left(S-a\right)$ matrix of coefficients are

$$
\begin{array}{cc}
m_{j,j}\left(a,t\right)=\left(R_{t+j}+1-\delta\right)e^{-f_{a+j,t+j}}+\Omega_{a+j,t+j}\frac{Z_{t+j}}{Z_{t+j-1}}e^{-f_{a+j-1,t+j-1}} & \text{if } 1\leq j\leq S-a\\
m_{j+1,j}\left(a,t\right)=-\Omega_{a+j+1,t+j+1}e^{-f_{a+j,t+j}}\left(R_{t+j}+1-\delta\right) & \text{if } 1\leq j<S-a\\
m_{j,j+1}\left(a,t\right)=-\frac{Z_{t+j+1}}{Z_{t+j}}e^{-f_{a+j,t+j}} & \text{if } 1\leq j<S-a\\
m_{j,j'}\left(a,t\right)=0 & \text{all other entries}
\end{array}
.
$$

The elements of $\mathbf{\Psi}\left(a,t\right)$ are

$$
\psi_j\left(a,t\right)=\begin{cases}
\begin{array}{c}
\Omega_{a+1,t+1}e^{-f_{a,t}}e_{a,t}\tilde{W}_t-e^{-f_{a+1,t+1}}e_{a+1,t+1}\tilde{W}_{t+1}\\
+\Omega_{a+1,t+1}\left(R_t+1-\delta\right)e^{-f_{a,t}}\phi\tilde{\Xi}_t\\
-\left(R_{t+1}+1-\delta\right)e^{-f_{a+1,t+1}}\phi\tilde{\Xi}_{t+1}\\
+\left(1-\Omega_{a+1,t+1}\right)\bar{C}+\Omega_{a+1,t+1}\left(R_t+1-\delta\right)\tilde{K}_{a,t}
\end{array} & \text{if } j=1\\
\begin{array}{c}
\Omega_{a+j,t+j}e_{a+j-1,t+j-1}e^{-f_{a+j-1,t+j-1}}\tilde{W}_{t+j-1}\\
-e_{a+j,t+j}e^{-f_{a+j,t+j}}\tilde{W}_{t+j}\\
+\Omega_{a+j,t+j}\left(R_{t+j-1}+1-\delta\right)e^{-f_{a+j-1,t+j-1}}\phi\tilde{\Xi}_{t+j-1}\\
-\left(R_{t+j}+1-\delta\right)e^{-f_{a+j,t+j}}\phi\tilde{\Xi}_{t+j}\\
+\left(1-\Omega_{a+j,t+j}\right)\bar{C}
\end{array} & \text{if } 1<j\leq A-a
\end{cases}
.
$$

Figure 1: Expected real return on 10-year zero-coupon Treasury security

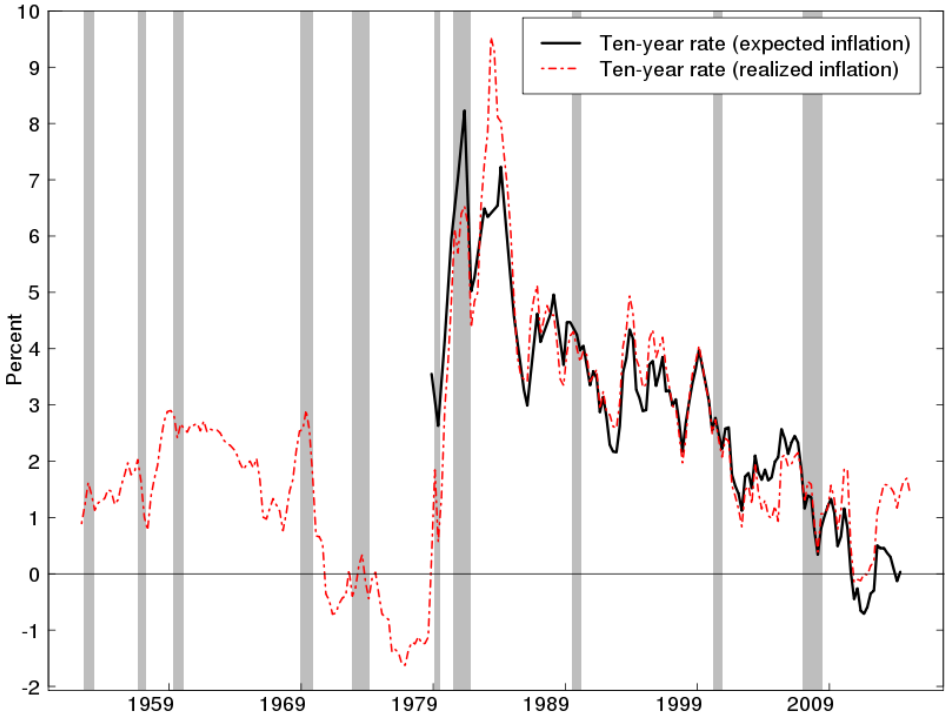

Source: Authors' calculation using data from FRED and Mertens and Nason (2015).
Notes: The "Ten-year rate (expected inflation)" is the difference between the zero-coupon ten-year nominal Treasury yield and an estimate of the expected ten-year CPI rate compute by Mertens and Nason (2015). This estimate amalgamates data from the Livingston Survey, the Survey of Professional Forecasters, and the Blue Chip Survey, The "Ten-year rate (realized inflation)" deflates the nominal yield series using a centered five-year moving average of realized quarterly CPI inflation. The shaded vertical bars represent periods of economic contraction, as identified by the NBER Business Cycle Dating Committee.

Figure 2: Johannsen and Mertens' (2016) smoothed estimate of the expected real interest rate in the long run

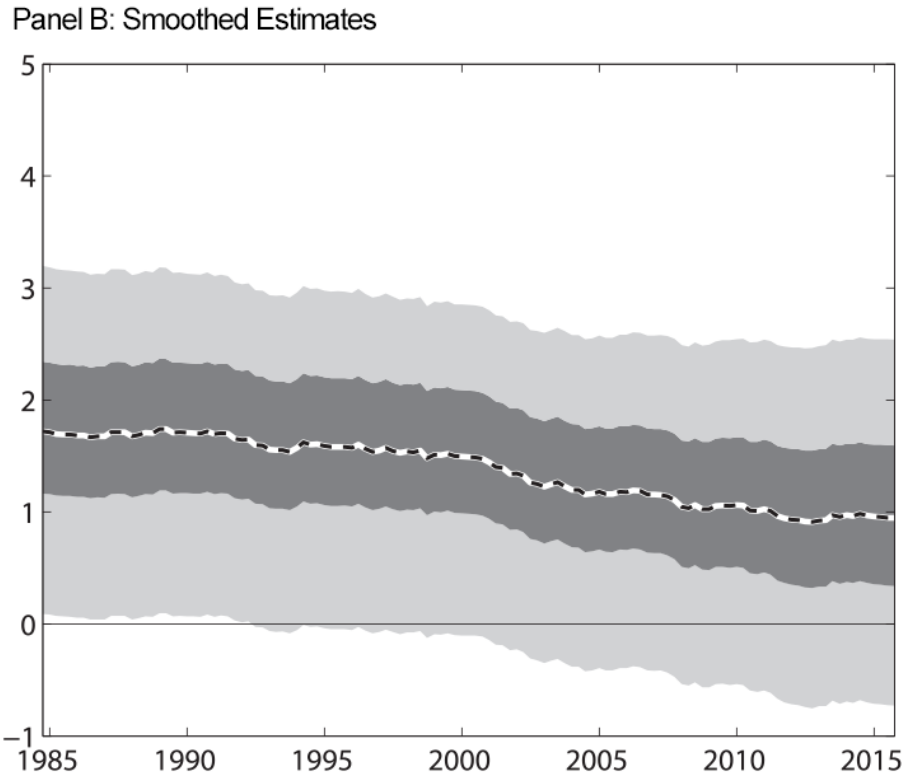

Source: Johannsen and Mertens (2016a).
Notes: These estimates use data through the entire sample to estimate the parameters and the historical level of the long-run real federal funds rate. The authors impose that the shadow rate be less than zero during the period in which the effective lower bound was binding. The shaded regions are 50 and 90 percent uncertainty bands. The estimated trend is expressed in annual percentage terms.

Figure 3: Yearly employment rates by age

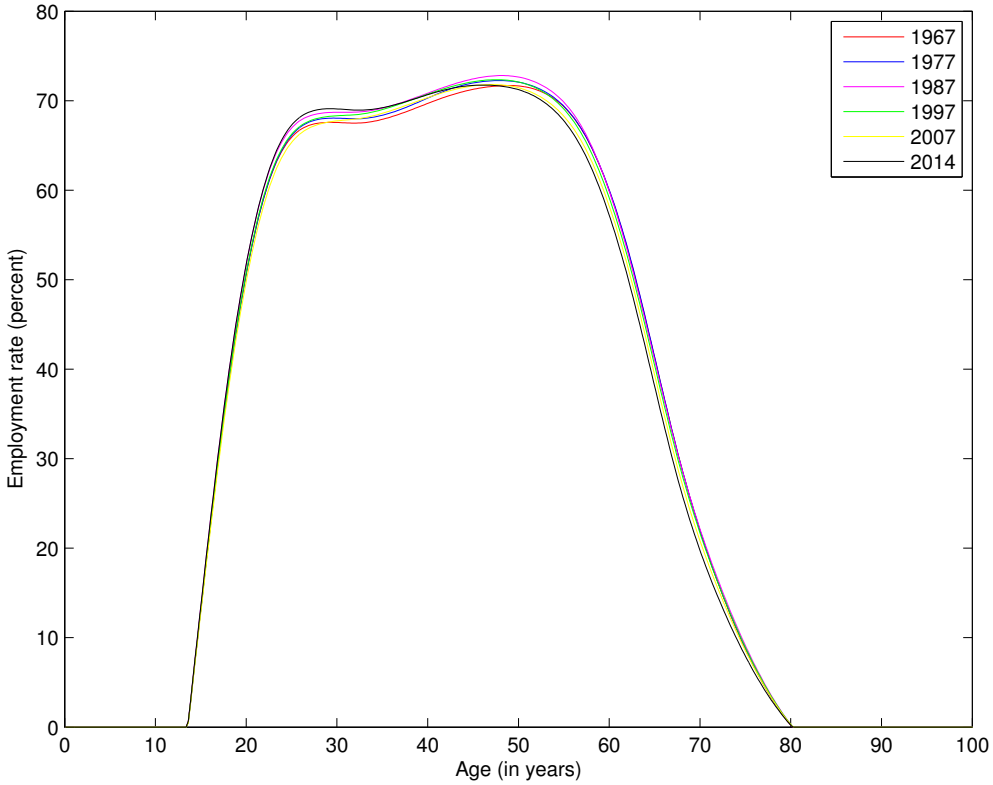

Source: Authors' interpolation of data from the U.S. Bureau of Labor Statistics.
Notes: The figure shows U.S. employment rates conditional on age. The underlying BLS data begin in 1967 and are for five-year age bins. The data shown are an interpolation to a quarterly frequency using cubic splines.

Figure 4: Annual live birth estimates and projections: 1900 to 2100

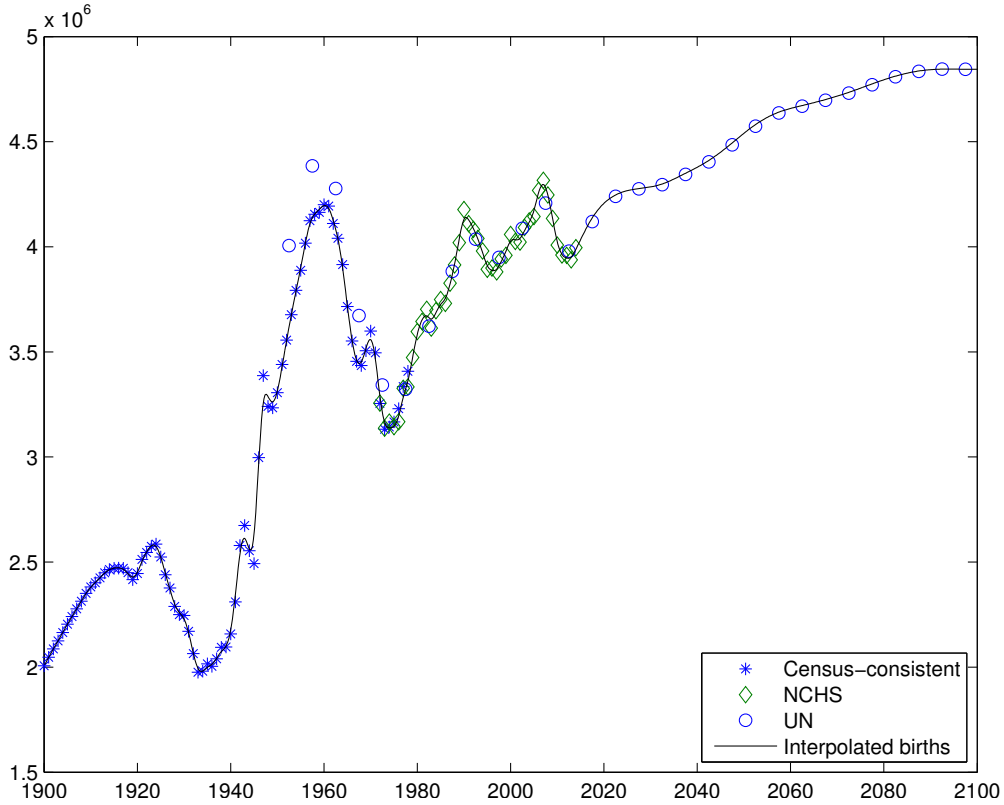

Source: Authors' calculations using data from the National Center for Health Statistics (NCHS), the United Nations' *World Population Prospects: Revision 2015* (WPP), and the U.S. Census Bureau.

Notes: We construct a historical birth series by stitching yearly estimates from the U.S. Census Bureau for the 1900–1971 period, yearly estimates from NCHS for 1972–2014 period, and five-year forecasts from the WPP estimates. The solid line shows our interpolation.

Figure 5: Estimated U.S. resident population at the turn of 1900

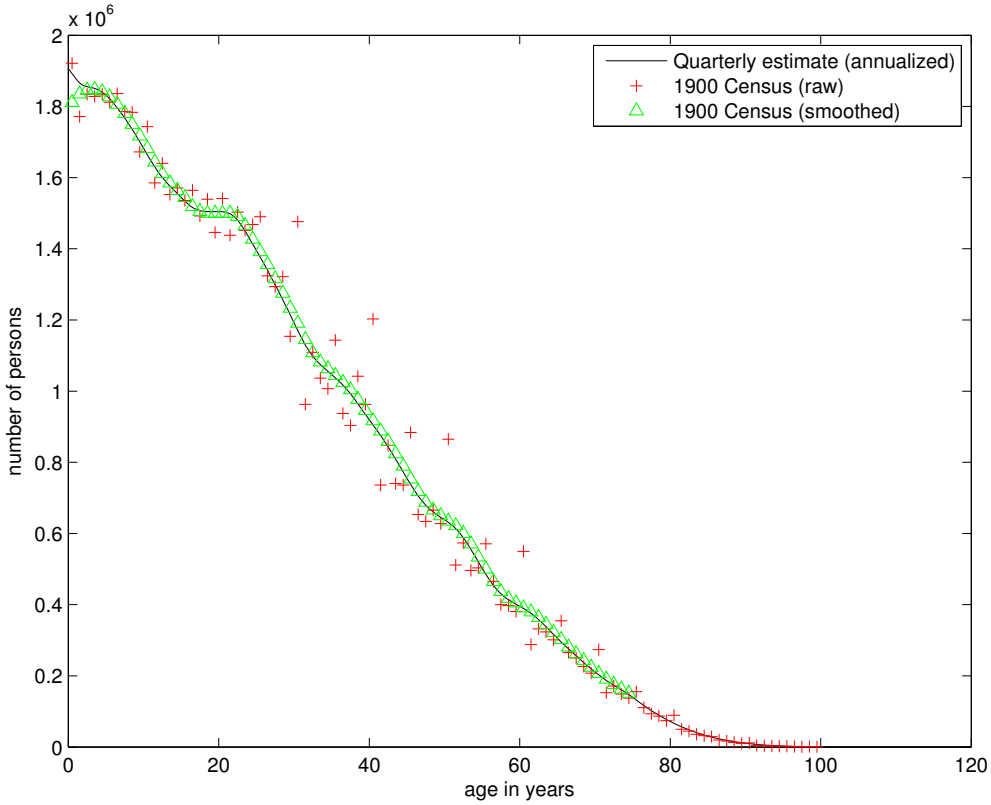

Source: U.S. Census Bureau, Bell and Miller (2005), and authors' calculations.
Notes: The stars and triangles in the figure show U.S. population estimates at the turn of 1900 by years of age based on the U.S. Census Bureau's raw estimates and smoothed estimates, respectively, of 1900 population census. We adjusted the mid-year figures to a turn-of-the-year basis using our interpolation of mortality rates from Bell and Miller (2005). The solid line shows our interpolation.

Figure 6: Share of births by age of mother (in years)

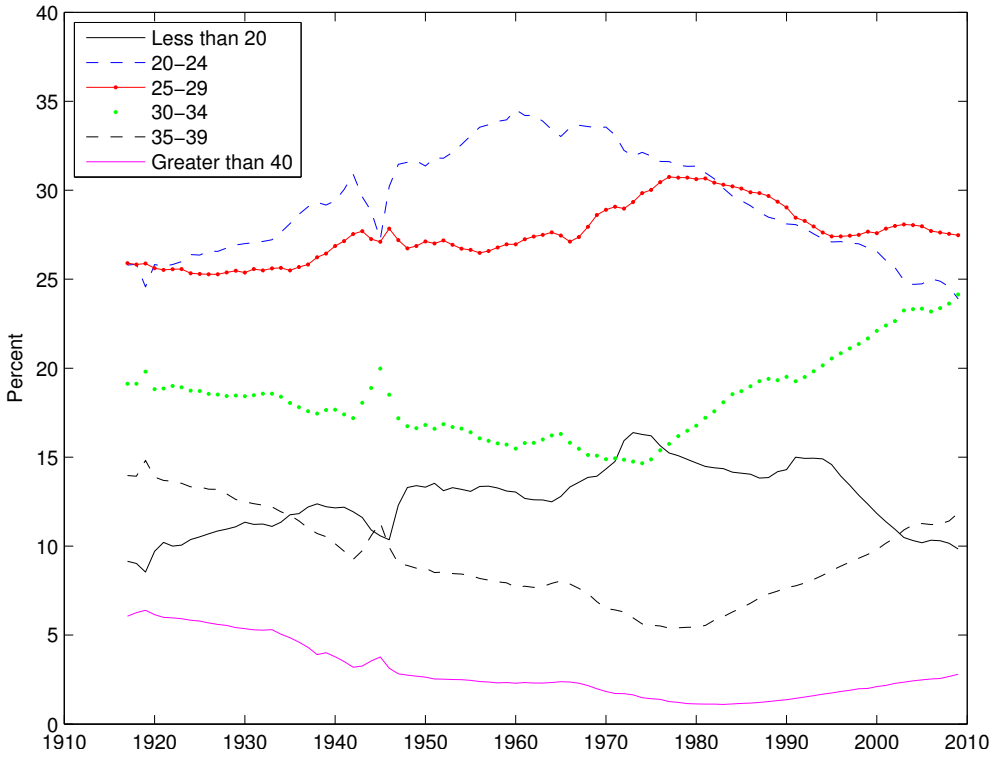

Source: Authors' calculations using U.S. data from Hamilton and Cosgrove (2010).

Figure 7: Median age difference between men and women at time of first marriage

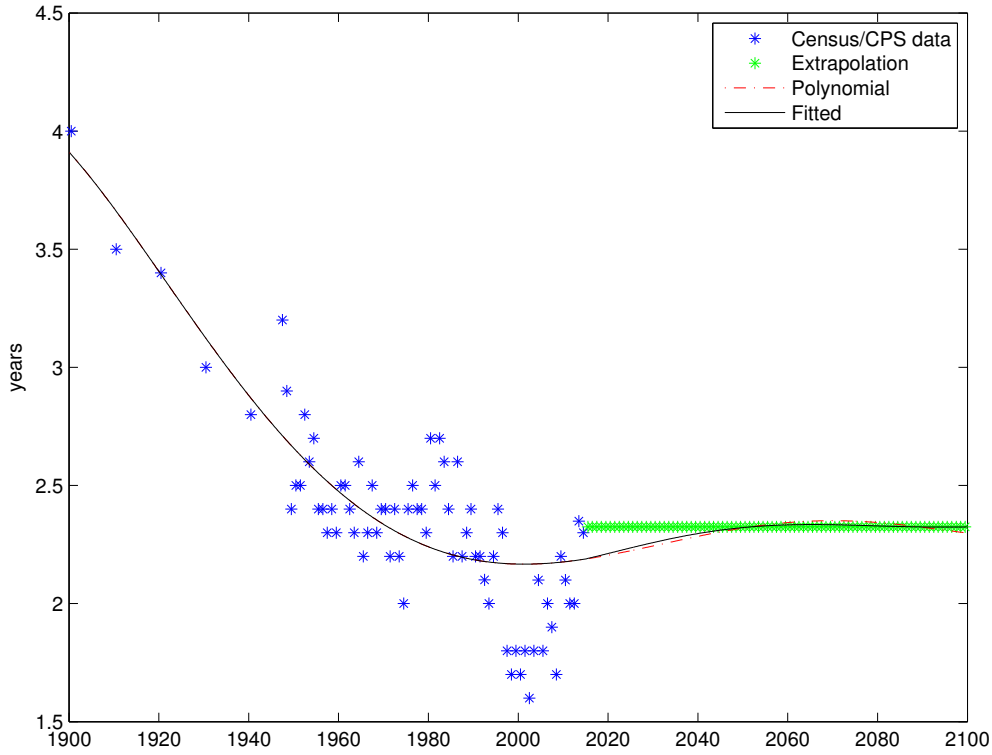

Source: Authors' calculations using from Hamilton and Cosgrove (2010), the U.S. Census Bureau's *Current Population Survey*.

Notes: Our interpolation assumes that the median age difference between men and women at the time of first marriage, averaged in 2013 and 2014, prevails in all subsequent periods.

Figure 8: Average number of dependent children by age and cohort of the representative parent

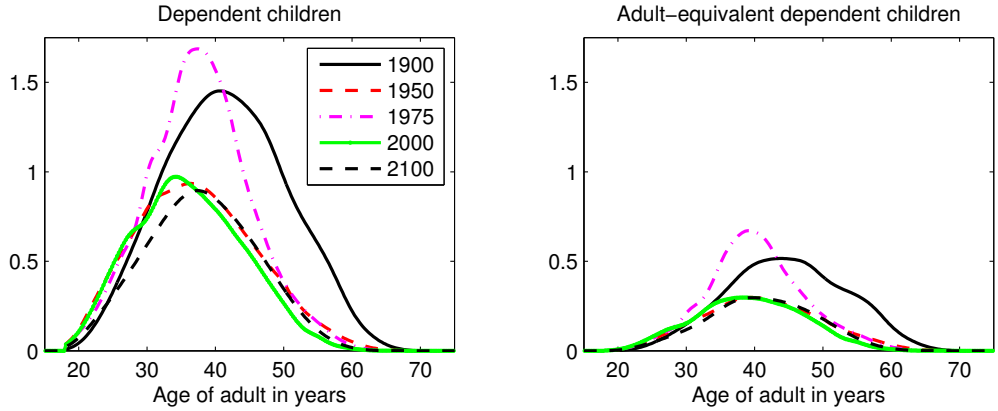

Source: Authors' calculations using data from U.S. Census bureau, Hamilton and Cosgrove (2010), the National Center for Health Statistics, the United Nations' *World Population Prospects: Revision 2015*, and the U.S. Census Bureau.

Notes: The number of adult-equivalent children consumers is calculated based on Browning and Ejrnæs' (2009) point estimates for their "more educated" household units.

Figure 9: Balanced growth and the equilibrium real rate

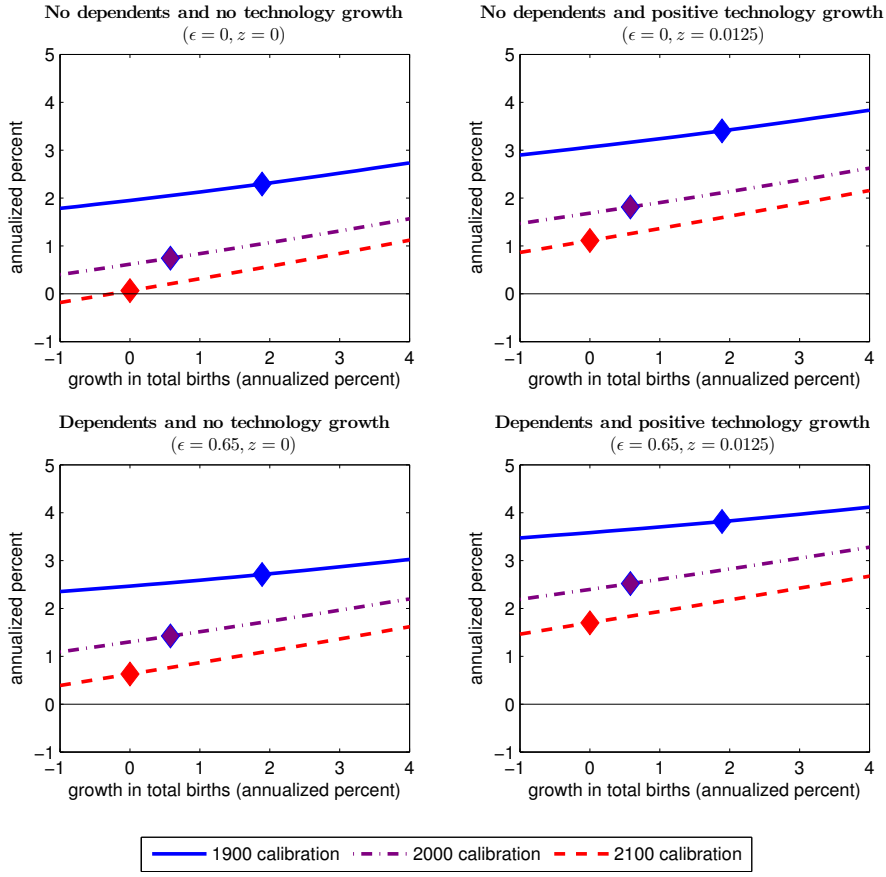

Source: Authors' model simulations.

Notes: The panels show the equilibrium real rate as a function of steady-state population growth for three sets of mortality tables (1900, 2000, and 2100) and various combinations of technology growth and assumption about children consumption. The diamonds indicate the steady-state results for the population growth that either was observed or is projected in the three reference years.

Figure 10: Consumption/saving decisions in the 2000 calibration of the steady state without technology growth

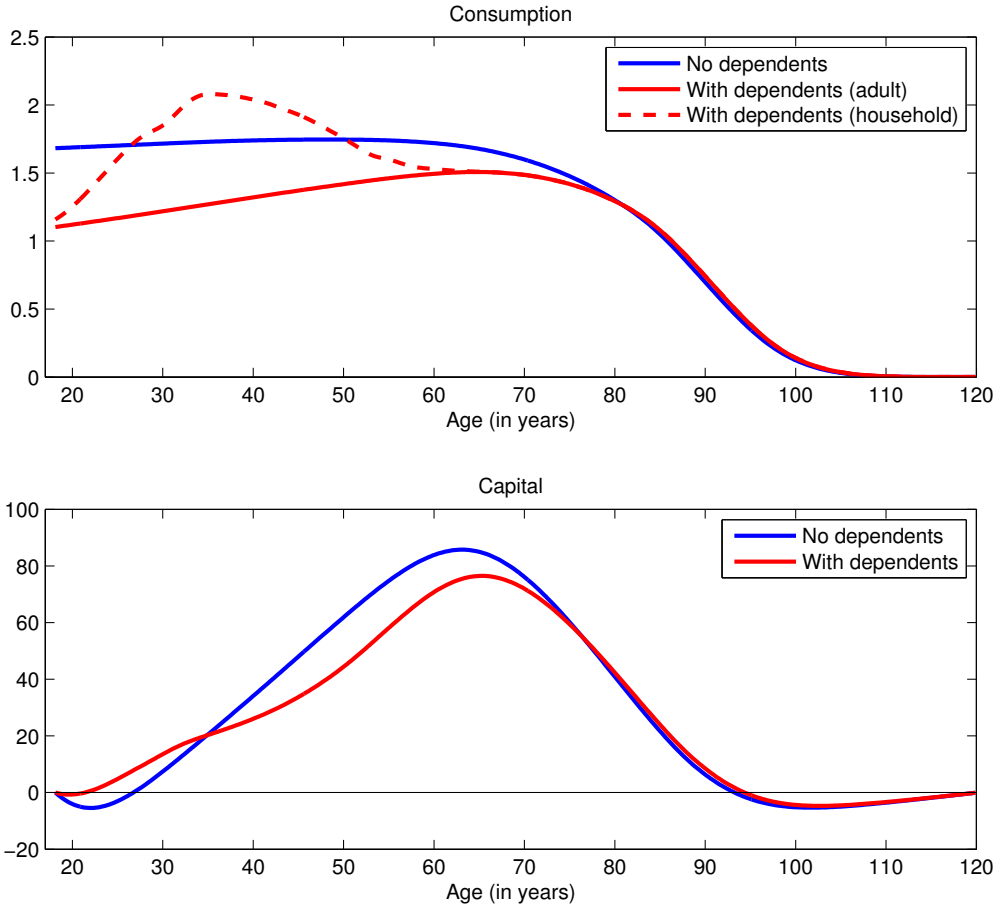

Source: Authors' model simulations.
Notes: The panels show the equilibrium real rate as a function of steady-state population growth for three sets of mortality tables (1900, 2000, and 2100) and various combinations of technology growth and assumption about children consumption. The diamonds indicate the steady-state results for the population growth that either was observed or is projected in the three reference years.

Figure 11: Equilibrium real rate in a balanced growth steady state with population and technology growth

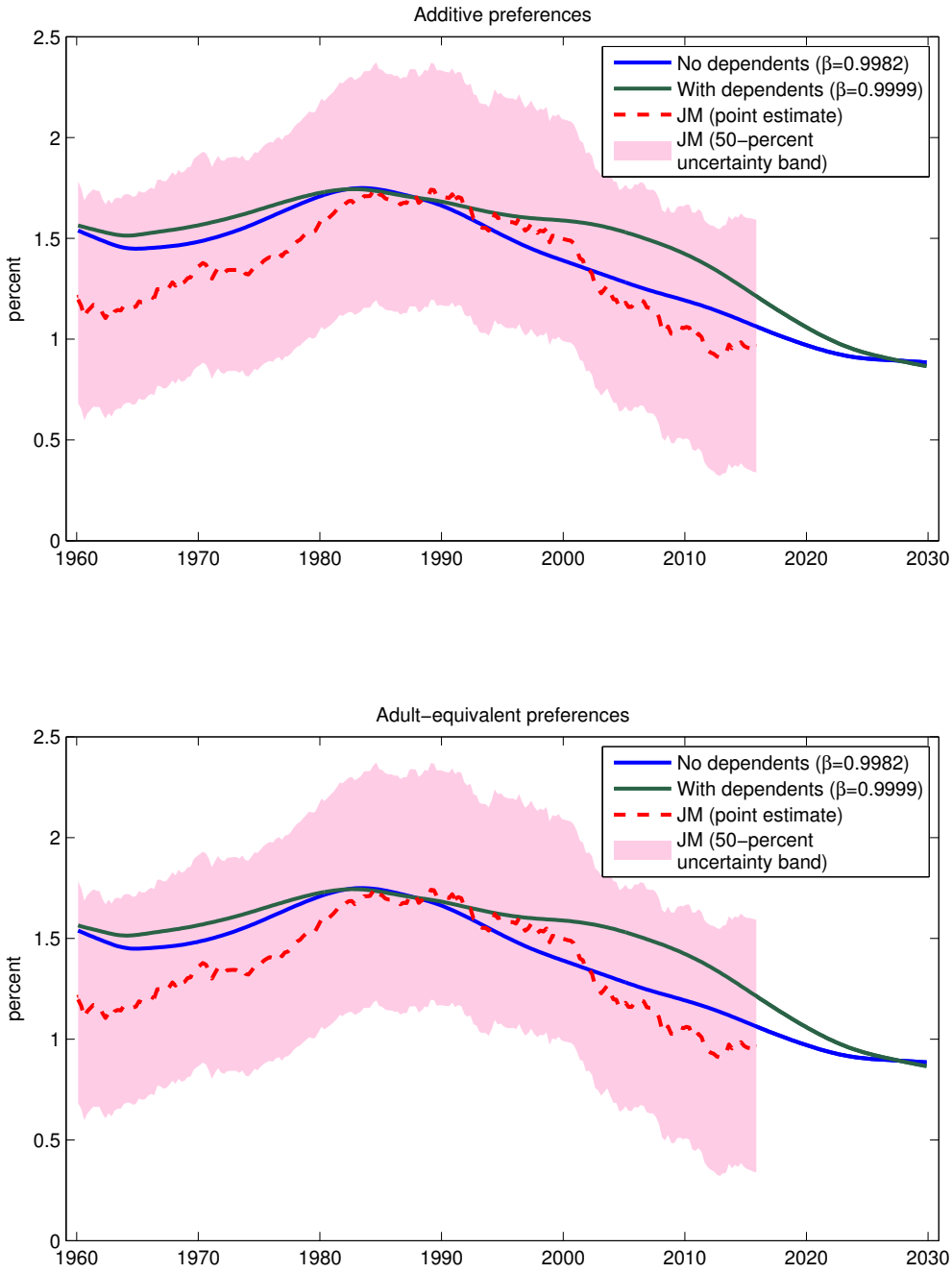

Source: Johannsen and Mertens (2016) and authors' calculations.

Notes: The figure shows the short-term equilibrium real rate in dynamic simulations of our model. The upper and lower panels use versions of the model in which the consumption of dependent children enters the utility of their representative parent additively and in adult-equivalent form, respectively. Each panel shows results with and without dependent children. The results are shown against Johannsen and Mertens' (2016) smoothed estimates of the expected real interest rate in the long run.

Figure 12: Dynamic simulation of life-cycle model with age-specific death rates, employment rates, and dependents

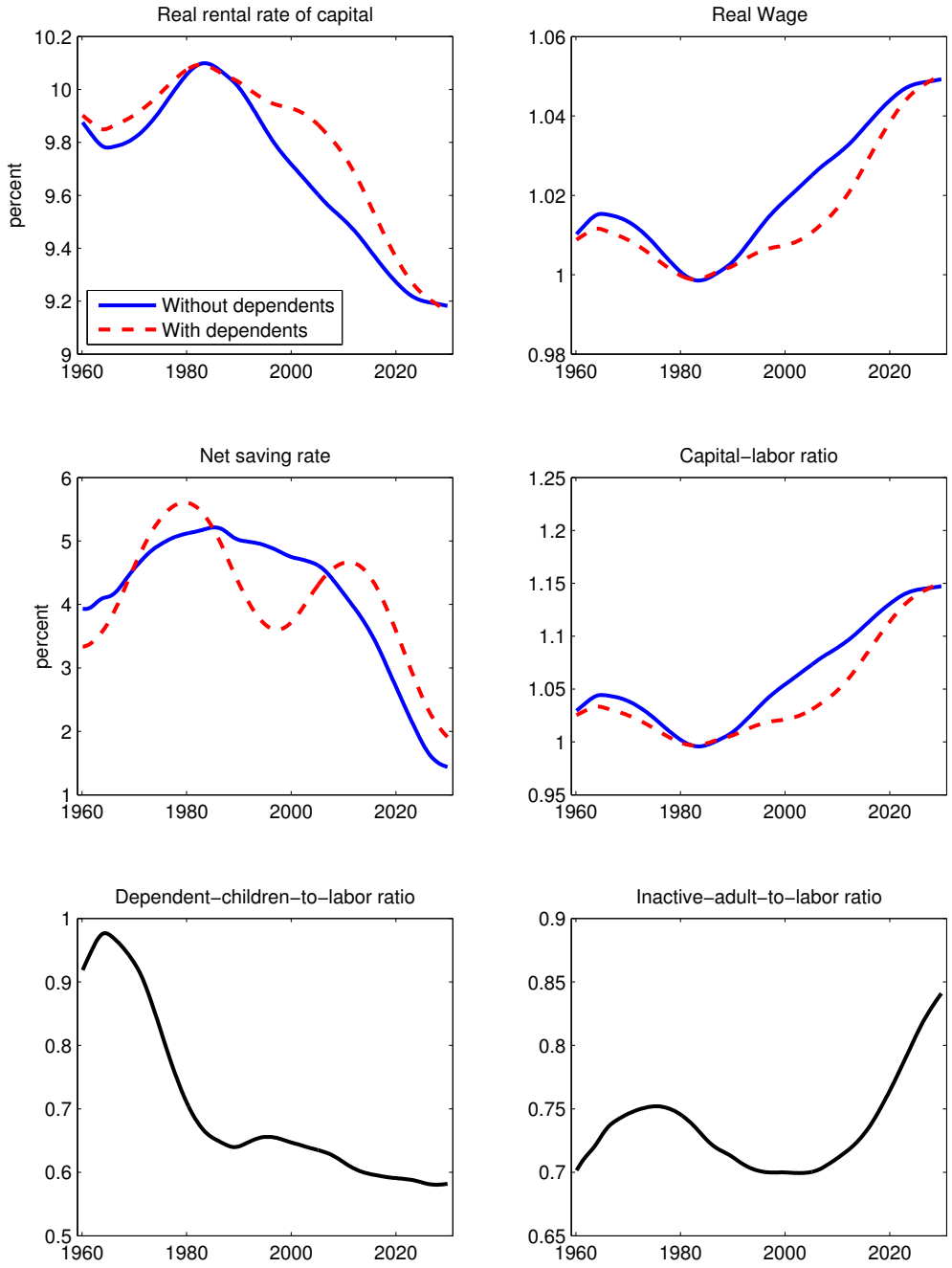

Source: Authors' calculations.

Notes: The lines labeled "Without dependents" and "With dependents" show simulation results under the assumption that representative adults receive no utility from their children's consumption and receive utility through an additive term, respectively. The real wage and the capital-labor ratio are scaled so that their level averages 1 in the 1980s. The bottom-left panel shows the number of dependent children scaled by the number of full-time equivalent labor endowments. The bottom-right panel shows the number of full-time equivalent adults who are inactive scaled by the number of full-time equivalent labor endowments.

Figure 13: Equilibrium real rate with constant mortality rates from 1960 onward

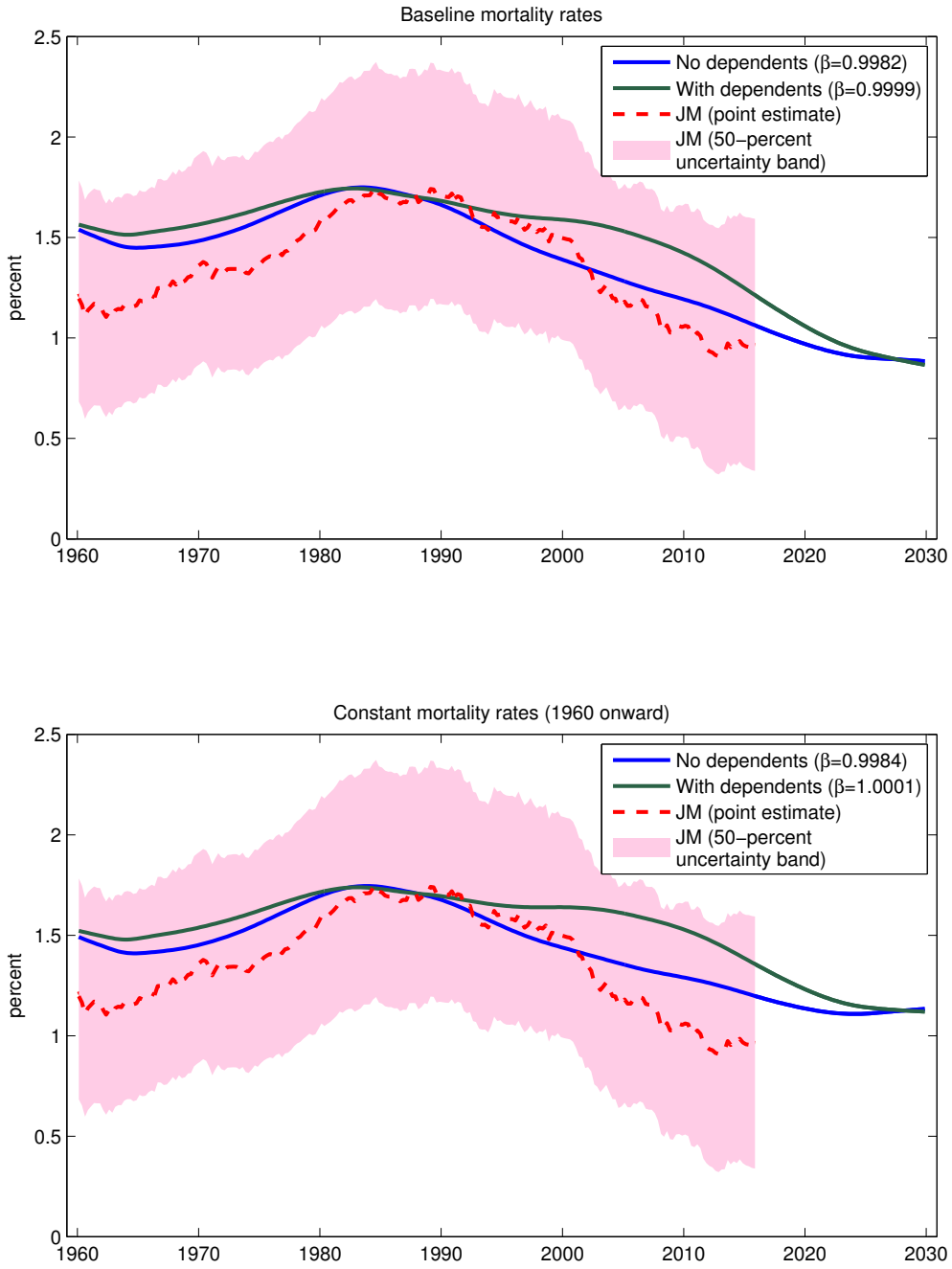

Source: Johannsen and Mertens (2016) and authors' calculations.

Notes: The figure shows the short-term equilibrium real rate in dynamic simulations of our model under the assumption that mortality rates from 1960:Q1 onward are held at the 1959:Q4 levels. The upper and lower panels use versions of the model in which the consumption of dependent children enters the utility of their representative parent additively and in adult-equivalent form, respectively. Each panel shows results with and without dependent children. The results are shown against Johannsen and Mertens' (2016) smoothed estimates of the expected real interest rate in the long run.

Figure 14: U.S. versus global demographic changes

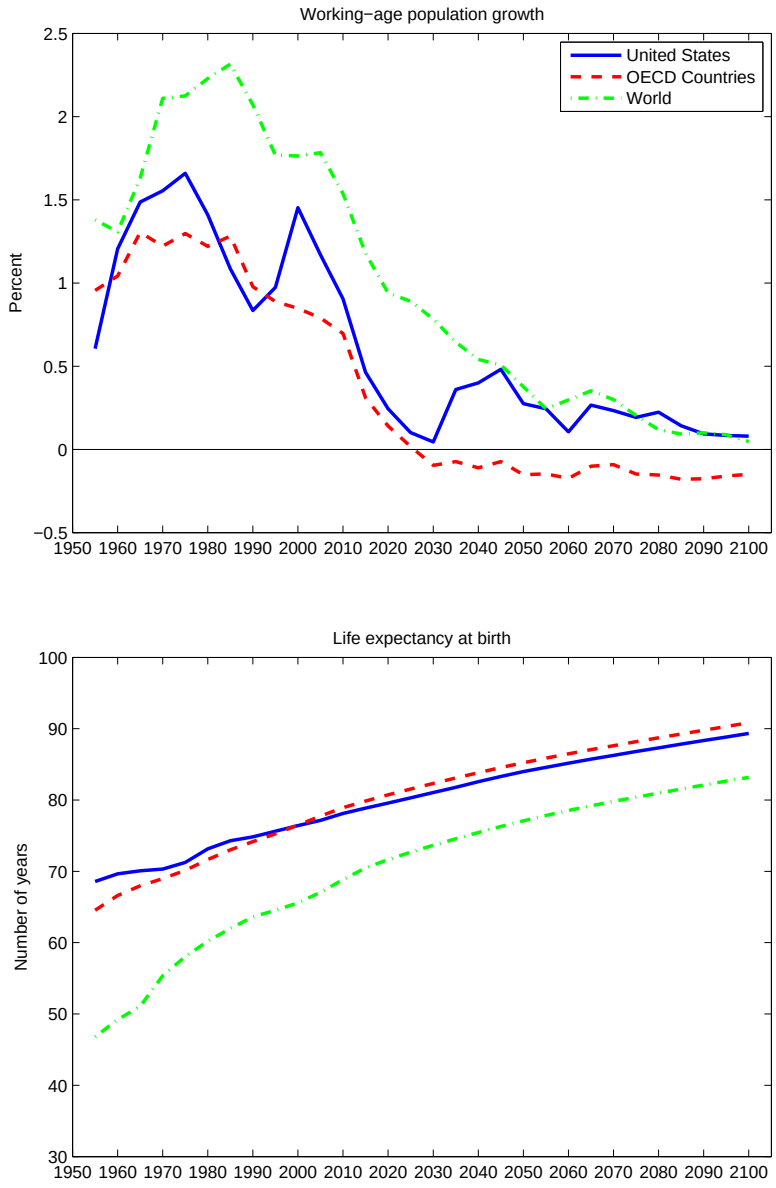

Source: Authors' calculations using data from the *World Population Prospects: Revision 2015* published by the United Nations.
Notes: The working-age population is defined as the set of individuals aged 15 to 64 years. We construct the OECD measure of mean life expectancy at birth as a population-weighted average of that statistic across OECD member countries.